



1 **All about Nitrite: Exploring Nitrite Sources and Sinks in the Eastern Tropical North**

2 **Pacific Oxygen Minimum Zone**

3

4 John C. Tracey^{1,2}, Andrew R. Babbin³, Elizabeth Wallace¹, Xin Sun^{1,4}, Katherine L. DuRussel^{1,}

5 ⁵, Claudia Frey^{1,6}, Donald E. Martocello III³, Tyler Tamasi³, Sergey Oleynik¹, and Bess B.

6 Ward¹

7

8 ¹ Department of Geosciences, Princeton University, Guyot Hall, Princeton, NJ, USA 08544

9 ² Department of Biology and Paleo Environment, Lamont Doherty Earth Observatory, Columbia
10 University, Palisades, NY, USA 10964

11 ³ Department of Earth, Atmospheric and Planetary Sciences, Massachusetts Institute of
12 Technology, Cambridge, MA, USA 02138

13 ⁴ Department of Global Ecology, Carnegie Institution for Science, Stanford, CA, USA 94305

14 ⁵ Department of Civil and Environmental Engineering, Northwestern University, Evanston, IL,
15 USA 60208

16 ⁶ Department of Environmental Sciences, University of Basel, Bernoullistrasse 30, 4056 Basel,
17 Switzerland

18

19 *Correspondence to:* John C. Tracey (jt16@alumni.princeton.edu)

20

21

22

23

24

25

26

27

28



29 **Abstract**

30 Oxygen minimum zones (OMZs), due to their large volumes of perennially deoxygenated
31 waters, are critical regions for understanding how the interplay between anaerobic and aerobic
32 nitrogen (N) cycling microbial pathways affects the marine N budget. Here we present a suite of
33 measurements of the most significant OMZ N cycling rates, which all involve nitrite (NO_2^-) as a
34 product, reactant, or intermediate, in the Eastern Tropical North Pacific (ETNP) OMZ. These
35 measurements and comparisons to data from previously published OMZ cruises present
36 additional evidence that NO_3^- reduction is the predominant OMZ N flux, followed by NO_2^-
37 oxidation back to NO_3^- . The combined rates of both of these N recycling processes were
38 observed to be much greater (up to nearly 200x) than the combined rates of the N loss processes
39 of anammox and denitrification, especially in waters near the anoxic / oxic interface. We also
40 show that NO_2^- oxidation can occur in functionally anoxic incubations, measurements that
41 further strengthen the case for truly anaerobic NO_2^- oxidation. We also evaluate the possibility
42 that NO_2^- dismutation provides the oxidative power for anaerobic NO_2^- oxidation. Although
43 almost all treatments returned little evidence for dismutation (as based on product inhibition,
44 substrate stimulation, and stoichiometric hypotheses), results from one treatment under
45 conditions closest to in situ NO_2^- values may support the occurrence of NO_2^- dismutation. The
46 partitioning of N loss between anammox and denitrification differed widely from stoichiometric
47 predictions of at most 29% anammox; in fact, N loss rates at many depths consisted entirely of
48 anammox. Through investigating the magnitudes of NO_3^- reduction and NO_2^- oxidation, testing
49 for anaerobic NO_2^- oxidation, examining the possibility of NO_2^- dismutation, and further
50 documenting the balance of N loss processes, these new data shed light on many open questions
51 in OMZ N cycling research.



52 **1. Introduction**

53 Nitrogen (N) is essential for life because of its prominent role in DNA, RNA, and protein
54 chemistry. As a result, N limits biological productivity in many marine environments. The
55 dissimilatory biological N loss and recycling pathways are traditionally understood to be strictly
56 separated by O₂ tolerance. The N loss processes of denitrification, the stepwise reduction of
57 NO₃⁻ to N₂, and anaerobic ammonium oxidation (anammox), the oxidation of NH₄⁺ with NO₂⁻ to
58 make N₂, require low O₂ while the N recycling pathways of NH₄⁺ oxidation to NO₂⁻ and NO₂⁻
59 oxidation to NO₃⁻ are viewed as obligately aerobic. Importantly, NO₂⁻ is a product, reactant, or
60 intermediate in all these pathways. Therefore, developing an understanding of NO₂⁻ sources and
61 sinks is essential for a complete understanding of marine N biogeochemistry.

62 Oxygen minimum zones (OMZs) and sediments are the two main marine environments
63 where N loss occurs. There are three major OMZs, the Eastern Tropical North Pacific (ETNP),
64 the Eastern Tropical South Pacific (ETSP), and the Arabian Sea, which occupy 0.1 - 1% of total
65 ocean volume, depending on the O₂ threshold used (Codispoti and Richards, 1976; Naqvi, 1987;
66 Bange et al., 2000; Codispoti et al., 2005; Lam and Kuypers, 2011). Importantly, the OMZ water
67 column is not completely deoxygenated from top to bottom; OMZs are characterized by an
68 oxygenated surface, a depth interval of steeply declining O₂ around the mixed layer depth, called
69 the oxycline, an oxygen deficient zone (ODZ) spanning several hundred meters where O₂
70 declines below the detection limit of common shipboard CTD O₂ sensors, and then a second,
71 gradual, oxycline that transitions to oxygenated deep water. Despite OMZ regions' small size,
72 they are responsible for 20-40% of total marine N loss (Brandes and Devol, 2002; Codispoti,
73 2007; Gruber, 2004), a magnitude significant for the global marine N budget. In this work, in
74 order to answer several open questions about OMZs and marine N cycling, we conducted a suite



75 of ^{15}N stable isotope measurements of the most important N cycling microbial pathways in
76 OMZs. We report the N loss rates of anammox and denitrification, as well as the N recycling
77 rates of NO_3^- reduction, NO_2^- oxidation, and NH_4^+ oxidation, all of which involve NO_2^- .

78 A distinctive feature of OMZs is a secondary nitrite maximum (SNM) (Codispoti et al.,
79 2001; Brandhorst, 1959; Codispoti and Packard, 1980). The highest nitrite concentrations within
80 the SNM can reach $10\ \mu\text{M}$, much higher than the peak values found in the primary nitrite
81 maximum at the base of the photic zone, which average $\sim 100\ \text{nM}$ globally (Lomas and
82 Lipschultz, 2006). Several recent works have shown or argued that the SNM's NO_2^- is supplied
83 via high rates of the first step of denitrification, NO_3^- reduction to NO_2^- (Lam et al., 2009; Lam
84 and Kuypers, 2011; Kalvelage et al., 2013; Babbin et al., 2017, 2020). NO_3^- reduction has been
85 proposed (Anderson et al., 1982) to be one-half of a rapid loop where NO_3^- and NO_2^- are
86 recycled through simultaneously occurring NO_3^- reduction and NO_2^- oxidation. This loop has
87 been supported through experimental measurements of both rates (Babbin et al., 2017, 2020;
88 Kalvelage et al., 2013; Lipschultz et al., 1990). In this view, elevated NO_3^- reduction also
89 generates NH_4^+ , via organic matter (OM) remineralization, which enhances anammox at the
90 expense of denitrification in oxycline and upper ODZ waters (Babbin et al., 2020). In this study,
91 we conducted tests to further document this rapid loop's existence and role in enhancing
92 anammox.

93 Recent measurements of NO_2^- oxidation have returned significant rates from both the
94 oxycline and the ODZ, findings that challenge the paradigm that NO_2^- oxidation is an obligately
95 aerobic process. Evidence for high, widespread NO_2^- oxidation rates in low O_2 waters has
96 accumulated from direct rate measurements via ^{15}N tracers (Füssel et al., 2011; Lipschultz et al.,
97 1990; Peng et al., 2015, 2016; Ward et al., 1989; Kalvelage et al., 2013; Tsementzi et al., 2016;



98 Sun et al., 2017, 2021; Babbin et al., 2017, 2020), models (Buchwald et al., 2015), and ^{15}N
99 natural abundance measurements (Casciotti et al., 2013). Many explanations have been
100 proposed including microaerophilic nitrite oxidizing bacteria (NOB) adapted to low but non-zero
101 O_2 conditions (Penn et al., 2016; Bristow et al., 2016; Tsementzi et al., 2016; Bristow et al.,
102 2017) where the O_2 for these NOB is transiently supplied to previously deoxygenated waters by
103 (1) vertical or horizontal mixing of the ocean surface or nearby oxic water (Casciotti et al., 2013;
104 Tiano et al., 2014; Bristow et al., 2016; Ulloa et al., 2012) or (2) a cryptic O_2 cycle where low-
105 light adapted phototrophs produce O_2 that is consumed by NOB (Garcia-Robledo et al., 2017).

106 While these explanations could account for oxycline and ODZ top observations, they
107 cannot account for rigorously O_2 contamination controlled observations of NO_2^- oxidation in
108 waters from the deep, dark, and deoxygenated ODZ core (Babbin et al., 2020; Sun et al., 2021).
109 These ODZ core results are bolstered by sequencing data that show the presence of NOB
110 exclusive to the deoxygenated ODZ core (Sun et al., 2019) and ODZ core kinetics experiments
111 where O_2 inhibits NO_2^- oxidation (Sun et al., 2021). Here we build on these results by
112 performing ^{15}N tracer experiments across a gradient of O_2 concentrations, including functionally
113 anoxic (< 3 nM) O_2 concentrations where O_2 cannot play a significant biological or
114 biogeochemical role (Berg et al., 2022).

115 Anaerobic NO_2^- oxidation would require an alternative oxidant other than O_2 . Many
116 candidates have been proposed for this oxidant including IO_3^- (Babbin et al., 2017), Mn^{4+} , Fe^{3+}
117 (Sun et al., 2021), the anammox core metabolism (Sun et al., 2021), the observed reversibility of
118 the nitrite oxidoreductase enzyme (Wunderlich et al., 2013; Kemeny et al., 2016; Koch et al.,
119 2015; Buchwald and Wankel, 2022), and NO_2^- dismutation (Babbin et al., 2020; Füssel et al.,
120 2011; Sun et al., 2021). Due to multiple considerations such as very low IO_3^- in the ODZ core



121 (Moriyasu et al., 2020), low favorability of Mn^{4+} or Fe^{3+} mediated NO_2^- oxidation at marine pH
122 values (Luther, 2010), low anammox rates that do not explain the observed stoichiometry of
123 NO_2^- oxidation to anammox (Kalvelage et al., 2013; Babbin et al., 2020; Sun et al., 2021), and
124 uncertainty if the enzyme hypothesis can account for structural and phylogenetic differences in
125 the NXR of the four NOB genera (Buchwald and Wankel, 2022; Sun et al., 2019), we
126 conducted experiments to test the remaining most plausible hypothesis: NO_2^- dismutation.

127 NO_2^- dismutation (Eq. (R4)) is energetically favorable (Strohm et al., 2007; Van de
128 Leemput et al., 2011) although it has not been detected in nature. The reaction is proposed to
129 occur in three steps (Eq. (R1-3)) (Babbin et al., 2020) and possible enzymes for steps 2 and 3
130 (Eqs. (R2, R3)) have been found in ODZ core metagenomic reads and metagenome assembled
131 genomes (MAGs) (Padilla et al., 2016; Babbin et al., 2020). While these sequences were not
132 classified as NOB, they do indicate that parts of the pathway could occur in OMZs. If
133 discovered in OMZs, NO_2^- dismutation would be another N loss pathway, albeit one
134 indistinguishable from denitrification since the ^{15}N atoms in $^{30}\text{N}_2$ come from $^{15}\text{NO}_2^-$ in both
135 pathways. Here we evaluate the hypothesis that NO_2^- dismutation is a significant mechanism for
136 NO_2^- oxidation under low O_2 , by searching for product inhibition, the inhibition of both NO_2^-
137 oxidation and $^{30}\text{N}_2$ production (i.e. denitrification) in response to addition of NO_3^- , substrate
138 stimulation (increases in both $^{30}\text{N}_2$ production and NO_2^- oxidation in response to addition of
139 $^{15}\text{NO}_2^-$), and by comparing the NO_2^- oxidation to the produced $^{30}\text{N}_2$ ratio. A ratio near the 3:1
140 stoichiometry of dismutation ($3 \text{NO}_3^- : 1 \text{N}_2$, Eq. (R4)) would indicate that dismutation could
141 explain the NO_2^- oxidation measured in the ODZ core.





146 A final area of OMZ biogeochemistry that we investigate is the relative balance between
147 anammox and denitrification and these pathways' relationships to the rapid NO_2^- oxidation /
148 NO_3^- reduction loop. After the discovery of anammox, many OMZ studies (Kalvelage et al.,
149 2013; Kuypers et al., 2005; Hamersley et al., 2007; Jensen et al., 2011; Thamdrup et al., 2006;
150 Lam et al., 2009), but not all (Ward et al., 2009; Bulow et al., 2010; Dalsgaard et al., 2012) have
151 reported that anammox is the dominant N loss flux in OMZs, a surprising difference from the
152 stoichiometric based prediction that OMZ N loss should be at most 29% anammox (Dalsgaard et
153 al., 2003). This prediction assumes that all NH_4^+ for anammox was derived from
154 remineralization of OM with a mean marine C:N ratio through complete denitrification of NO_3^-
155 to N_2 (Dalsgaard et al., 2003, 2012). Anammox rates exceeding 29% of total N loss would
156 therefore require an additional source of NH_4^+ beyond current observations of denitrification and
157 the resulting NH_4^+ remineralization. The best supported explanations for elevated anammox are
158 that (1) denitrification is the NH_4^+ source, but that complete denitrification peaks episodically in
159 response to OM quality while anammox occurs at a slow, consistent, low rate (Ward et al., 2008;
160 Thamdrup et al., 2006; Babbin et al., 2014; Dalsgaard et al., 2012). The snapshots afforded by
161 isotopic incubations on cruises could therefore easily miss episodes of high complete
162 denitrification. (2) The rapid loop between NO_3^- and NO_2^- described previously functions as an
163 "engine" to generate NH_4^+ for anammox at the expense of denitrification. The observed
164 magnitudes of NO_3^- reduction and NO_2^- oxidation and these processes' ability to produce NH_4^+
165 from the remineralization of OM with standard C:N ratios without complete denitrification make
166 this an additional logical hypothesis.

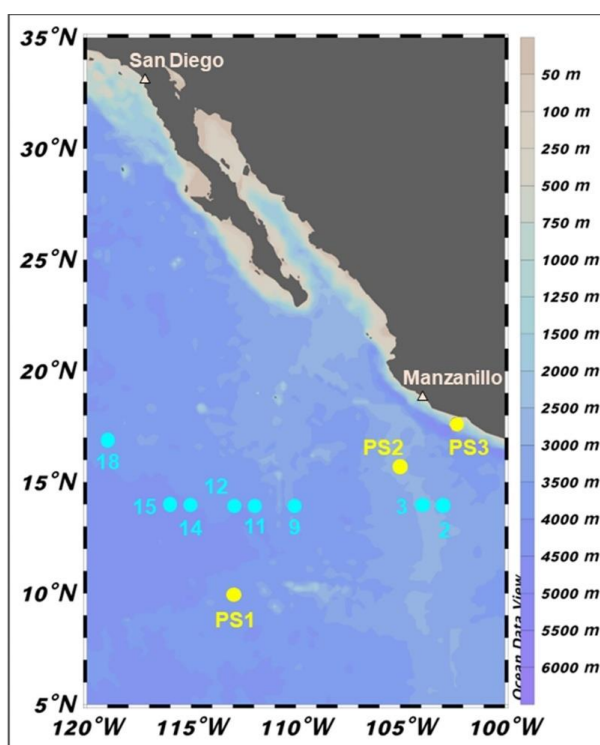


167 The second hypothesis is supported by several pieces of evidence such as (1)
168 measurements that the O₂ tolerance of NO₃⁻ reduction and anammox is higher than that of
169 denitrification and that therefore these processes are more adapted to the oxycline and ODZ top
170 (Kalvelage et al., 2011; Jensen et al., 2008; Dalsgaard et al., 2014). Additionally, (2) ‘omics
171 studies have revealed widespread incomplete, modular denitrification in OMZs (Sun and Ward,
172 2021; Ganesh et al., 2015; Fuchsman et al., 2017), and (3) experimental studies have shown that
173 as NO₃⁻ reduction increases near the coast, anammox rates also increase (Kalvelage et al., 2013).
174 According to this view, partial denitrification of NO₃⁻ to NO₂⁻ at a much higher rate than
175 complete denitrification would produce NH₄⁺ that would then enhance anammox rates. The
176 resulting enhanced anammox rates occur at the expense of complete denitrification because high
177 NO₃⁻ reduction rates would consume OM before the later steps of denitrification. In addition, the
178 resulting NO₂⁻ would also be lost to later stage denitrifiers due to high NO₂⁻ oxidation rates that
179 would return the NO₂⁻ to NO₃⁻. Our study’s considerable number of data points, as well as our
180 ability to compare results to rate measurements obtained from identical methods on previous
181 cruises offers a unique chance to further validate these explanations for elevated anammox rates.

182 OMZs are essential regions for the marine N cycle; however, the biogeochemistry of
183 OMZs may currently be in flux due to anthropogenic pressures. Models and observations
184 suggest that OMZ volume will grow in the near future, with uncertain impacts (Stramma et al.,
185 2008; Keeling et al., 2010; Horak et al., 2016; Busecke et al., 2022). As a result, it is important
186 to develop a thorough understanding of OMZ N cycling to be able to predict any changes in
187 marine productivity as deoxygenated regions grow. This study contributes towards this goal
188 through examining four open research questions in OMZ biogeochemistry:



- 189 (1) Is the rapid cycle hypothesis correct, i.e., that NO_3^- reduction and NO_2^- oxidation rates are
190 much greater than N loss rates, especially in the oxycline and ODZ top?
191 (2) Does truly anaerobic NO_2^- oxidation occur in OMZ regions?
192 (3) If yes, is NO_2^- dismutation the mechanism by which it occurs?
193 (4) Is anammox the dominant N loss flux? If yes, what is the explanation?



194

195 **Figure 1:** Sampling locations during 2018 cruises to the ETNP OMZ. SR1805 stations (spring
196 2018) are shown in yellow while FK180624 (summer 2018) stations are shown in cyan. Stations
197 PS1 and 18 are located in more oxic environments on the boundary of the OMZ region. The
198 remaining FK180624 stations occur along a gradient towards the center of the OMZ region,
199 represented by stations PS2 and FK180624 stations 2 and 3. These three stations are referred to
200 as OMZ core stations. Station PS3 (referred to as coastal) represents a final biogeochemical
201 subregion due to its proximity to the coast.

202

203 2. Methods

204 2.1 NO_2^- , NO_3^- , and NH_4^+ concentration measurements



205 Nutrient measurements on all cruises were conducted as follows. Ambient NO_2^-
206 concentrations were measured using the sulfanilimide and NED colorimetric technique with a
207 spectrophotometer (Strickland and Parsons, 1972). NO_3^- was measured in the NO_2^- oxidation
208 experiments using the chemilumescence method (Braman and Hendrix, 1989). Ambient NH_4^+
209 concentrations were measured using the OPA method (Holmes et al., 1999; Taylor et al., 2007;
210 ASTM International, 2006). In some cases, NO_2^- and NH_4^+ were measured on different casts
211 than those of the rate measurements. In these cases, figures and calculations use interpolated
212 nutrient values based on the potential density of nutrient sampling and rate measurement depths.
213 Interpolations were performed with the Matlab `pchip` function.

214 **2.2 NH_4^+ oxidation and NO_3^- reduction rates**

215 Incubation experiments were performed on board the R/V *Sally Ride* in March and April
216 2018 (SR1805). NH_4^+ oxidation and NO_3^- reduction rates were measured at three stations: PS1
217 (open ocean OMZ boundary), PS2 (open ocean, OMZ), and PS3 (coastal OMZ) (Fig. 1). Rates
218 were measured throughout the water column at ten depths per station (see supplemental Table S1
219 for depths). Water was directly sampled from the CTD into 60-mL serum vials. After
220 overflowing three times, bottles were sealed with a rubber stopper and crimped with an
221 aluminum seal. A 3 mL headspace of He was introduced, samples from below the oxygenated
222 surface depths were purged for 15 min with He, and then 0.1 mL of tracer solution was added to
223 all bottles. $^{15}\text{NH}_4^+$ and $^{15}\text{NO}_3^-$ tracers were added to reach final concentrations of 0.5 μM and 3
224 μM , respectively. Five bottles were incubated per time course and incubations were ended at 0
225 (one bottle), 12, and 24 hours (two bottles each) via addition of 0.2 mL of saturated ZnCl_2 .
226 Samples were analyzed at the University of Basel using a custom-built gas bench connected by a
227 Conflow IV interface to a Delta V plus IRMS (Thermo Fisher Scientific). Five mL of the sample



228 were used to convert NO_2^- to N_2O using the azide method (McIlvin and Altabet, 2005). A linear
229 increase of $^{15}\text{N}\text{-NO}_2^-$ over time, along with a standard curve to convert from peak area units to
230 nmol N was used to calculate the NO_2^- production rates according to Eq. (5) and (6) below,

231 Ammonium oxidation rate =
$$\frac{d \text{ }^{15}\text{NO}_2^-}{dt (F_{\text{NH}_4^+})} \quad (5)$$

232 Nitrate reduction rate =
$$\frac{d \text{ }^{15}\text{NO}_2^-}{dt (F_{\text{NO}_3^-})} \quad (6)$$

233 where:

234 $\frac{d \text{ }^{15}\text{NO}_2^-}{dt}$ is the slope of $^{15}\text{NO}_2^-$ produced over time and

235 $F_{\text{NH}_4^+}$ and $F_{\text{NO}_3^-}$ are the fraction of the NO_3^- and NH_4^+ pools that are labelled with ^{15}N .

236 The significance of the rates was evaluated using a Student's t test with a significance level of
237 0.05. The reported error bars are the standard error of the regression. The NH_4^+ oxidation rates
238 reported here were previously published and the experimental method used is more thoroughly
239 described in this previous publication (Frey et al., 2022).

240

241 **2.3 Anammox and denitrification rates depth profiles**

242 Incubation experiments were performed during SR1805 in March and April 2018 and on
243 the R/V *Falkor* (FK180624) during June and July 2018. As above, rates were measured at PS1,
244 PS2, and PS3 at ten depths per station (see Supplementary Table S1 for sampling depths) during
245 SR1805. On FK180624, rates were measured at eight stations that spanned a gradient from the
246 core of the OMZ region to its edges (see Supplementary Table S2 for sampling depths). At all
247 stations and depths water was directly sampled from the CTD into 320 mL borosilicate ground
248 glass stoppered bottles. After overflowing three times, bottles were stoppered with precision



249 ground glass caps specifically produced to prevent gas flow. The bottles were transferred to a
250 glove bag and amended with the following treatments: 3 μM each of $^{15}\text{NO}_2^-$ and $^{14}\text{NH}_4^+$
251 (denitrification and anammox) and 3 μM each of $^{15}\text{NH}_4^+$ and $^{14}\text{NO}_2^-$ (anammox) on SR1805.
252 Two μM amendments of $^{15}\text{NO}_2^-$ and $^{14}\text{NH}_4^+$ were used on FK180624. Eight mL of tracer
253 amended seawater was aliquoted into 12-mL exetainers (Labco). Exetainers were sealed in a
254 glove bag with butyl septa and plastic screw caps that had been stored under helium for at least
255 one month, removed and then purged for 5 min at 3 psi with helium gas to remove any O_2 that
256 accumulated during sampling and processing. As a result of this step, it should be noted that all
257 anammox and denitrification rates sourced from partially or fully oxygenated waters represent
258 potential rates.

259 Rates for each sampled depth were calculated using a five-timepoint time course with
260 three replicates at each point. Incubations were ended by injecting 50 μL saturated ZnCl_2 and
261 vials were stored upside down to prevent the headspace from leaking through the vial cap in
262 storage and transit. Six months after the cruise, samples were analyzed using a Europa 22-20
263 IRMS (Sercon). Raw data values were corrected for instrument drift due to run position and
264 total N_2 mass. Drift corrected values and standard curves to convert from peak area units to
265 nmol N_2 were used to calculate rates according to the equations below (Thamdrup et al., 2006;
266 Thamdrup and Dalsgaard, 2000, 2002) (for more details see supplemental material),

267 Denitrification (from $^{15}\text{NO}_2^-$)

$$268 \text{ Denitrification Rate} = \frac{d \text{ } ^{30}\text{N}_2}{dt(F_{\text{NO}_2^-})^2} \quad (7)$$

269 Anammox (from $^{15}\text{NO}_2^-$)

$$270 \text{ Anammox Rate} = \frac{d \text{ } ^{29}\text{N}_2}{dt F_{\text{NO}_2^-}} - 2D(1 - F_{\text{NO}_2^-}) \quad (8)$$



271 Anammox (from $^{15}\text{NH}_4^+$)

$$272 \text{ Anammox Rate} = \frac{d \text{ }^{29}\text{N}_2}{dt F_{\text{NH}_4^+}} \quad (9)$$

273 where:

274 $\frac{d \text{ }^{30 \text{ or } 29}\text{N}_2}{dt}$ is the slope of the regression of the amount of $^{30 \text{ or } 29}\text{N}_2$ vs. time,

275 $F_{\text{NO}_2^-}$ and $F_{\text{NH}_4^+}$ are the fraction of the NO_2^- and NH_4^+ pools labelled as ^{15}N , and

276 D is the denitrification rate calculated according to Eq. (7).

277 A Student's t test with a significance level of 0.05 was used to evaluate all rates. The reported
278 error bars are the standard error of the regression. Since the anammox rates measured via both
279 tracers on the SR1805 cruise were similar in magnitude (Supplementary Table S3), anammox
280 values reported in Figs. 2, 3, 6, 7, 8, and 9 are based on a combination of these values (see
281 supplementary material for more information). Previously published (Babbin et al., 2020)
282 anammox and denitrification rates are sourced from four stations occupied during the R/V
283 *Thomas G. Thompson's* March and April 2012 cruise to the ETNP (TN278) and the RVIB
284 *Nathaniel B. Palmer's* June and July 2013 ETSP cruise (NBP1305) and were conducted in the
285 same manner as the SR1805 and FK180624 incubations. Station locations for these cruises were
286 as follows: TN278 ETNP coastal (20° 00' N, 106° 00' W), ETNP offshore (16° 31' N, 107° 06'
287 W) and NBP1305 ETSP coastal (20° 40' S, 70° 41' W), ETSP offshore (13° 57' S, 81° 14' W).

288

289 **2.4 SR1805 NO_2^- oxidation depth profiles**

290 Nitrite oxidation depth profiles were measured in the same exetainers used to measure
291 anammox and denitrification depth profiles ($^{15}\text{NO}_2^-$ treatment only). The rate of NO_2^- oxidation
292 was determined by converting the NO_3^- produced during the incubations to N_2O using the



293 denitrifier method (Weigand et al., 2016; Granger, J., & Sigman, 2009) (see supplemental
294 material for methods details). The samples were stored at room temperature in the dark until
295 analysis on a Delta V (Thermo Fisher Scientific) mass spectrometer that measures the isotopic
296 content of N in N₂O (Weigand et al., 2016). Samples were corrected for instrument drift due to
297 run position and total N₂ mass (for more details see supplemental materials). Drift corrected
298 $\delta^{15}\text{N}$ values and a standard curve were then used to calculate the rate as follows,

$$299 \quad \frac{^{15}\text{N}}{^{14}\text{N}} = \frac{\left[\frac{\delta^{15}\text{N}}{1000} + 1 \right] \times 0.003667}{1 - 0.003667} \quad (10)$$

$$300 \quad \text{NO}_2^- \text{ ox. rate} = \frac{d \left[^{44}\text{N}_2\text{O}_{\text{area}} \times \frac{^{15}\text{N}}{^{14}\text{N}} \right]}{dt F_{\text{NO}_2^-}} \quad (11)$$

301 where Eq. (10) is a rearrangement of the definition of $\delta^{15}\text{N}$:

$$302 \quad \delta^{15}\text{N} = \left[\frac{\frac{^{15}\text{N}}{^{14}\text{N}}_{\text{sample}}}{\frac{^{15}\text{N}}{^{14}\text{N}}_{\text{air}}} - 1 \right] \times 1000 \quad (12)$$

303 and $^{44}\text{N}_2\text{O}_{\text{area}}$ is the amount of $^{44}\text{N}_2\text{O}$ measured as sample peak area in V · sec. 0.003667 is the
304 natural abundance of ^{15}N in air. A Student's t test with a significance level of 0.05 was used to
305 evaluate all rates. Reported error bars are the standard error of the regression. Previously
306 published (Babbin et al., 2020) NO_2^- oxidation rates are from the previously mentioned TN278
307 and NBP1305 cruises and were conducted at the same four stations where N loss rates were
308 measured. These NO_2^- oxidation rate measurements were conducted according to the same
309 procedures used for the SR1805 depth profiles.

310

311 **2.5 NO_2^- oxidation and O_2 manipulation experiments**



312 Experiments were conducted during cruises SR1805 and FK180624 in spring and
313 summer 2018. Wide-mouthed Pyrex round media bottles (800 mL total volume, 500 mL
314 working volume; Corning, USA; product code 1397-500) were used for all incubations. These
315 bottles were modified to include three stainless steel bulkhead fittings (Swagelok, USA) secured
316 to the interior of the lid with a Viton rubber gasket and stainless-steel washer between the lid and
317 the sealing nut. The three ports consisted of two one-eighth inch fluidic ports (inflow and
318 outflow) and one one-quarter inch sampling port. The fluidic ports were fitted with one-eighth
319 inch nylon tubing, with the inflow line penetrating to the base of the bottle. The one-quarter inch
320 sampling port had a butyl rubber septum between the Swagelok stem and nut. This setup
321 permitted *continuous* gas purging of the bottles while maintaining an otherwise closed system.

322 For each depth and O₂ treatment, three bottles were filled to 500 mL with sample water
323 and closed. Highly precise digital mass flow controllers (Alicat) were used to establish O₂
324 concentrations in each bottle. Mixing ratios were calculated to create a range of O₂
325 concentrations spanning 1 nM, 10 nM, 100 nM, 1 μM, and 10 μM. The gas mixture modified by
326 the mass flow controllers was a zero-air gas mixture (Airgas) consisting of 21% O₂ and 79% N₂
327 and 1000 ppm pCO₂ (the approximate in situ value). Initial gas flow was 1 L min⁻¹ for 1 hour to
328 equilibrate the seawater followed by 100 mL min⁻¹ for the remainder of the experiment. Bottles
329 were daisy-chained together to maintain the same flow rate among them (two bottles on SR1805,
330 six on FK180624). As in the depth profile experiments, 3 μM ¹⁵NO₂⁻ amendments were added
331 prior to purging. Incubations were conducted in the dark at 12°C in a cold room (SR1805) or
332 beverage cooler (FK180624). At the beginning of the experiments, after purging for one hour,
333 O₂ was checked with a LUMOS optode with a detection limit of 0.5 nM (Lehner et al., 2015) and
334 CO₂ was checked by measuring pH using the colorimetric meta-cresol purple method. The



335 LUMOS optode confirmed that O₂ concentrations were within a few nM of the calculated values.
336 While our use of high precision digital mass flow controllers and this qualitative O₂ check
337 provide confidence that our O₂ concentrations are accurate, due to the fact that O₂ was not
338 continuously monitored through the time course, we refer to each O₂ concentration as a
339 “putative” concentration. Samples (50 mL) were withdrawn every 12 hours for two days with a
340 four inch hypodermic needle attached to a 60 mL disposable plastic syringe. Samples were
341 ejected into acid-cleaned HDPE bottles pre-amended with 200 μL of saturated ZnCl₂ solution.
342 Bottles were screwed closed and wrapped with parafilm. Samples from each of the three initially
343 collected bottles were collected to create triplicates at each time point.

344

345 **2.6 NO₂⁻ dismutation experiments**

346 Nitrite dismutation experiments were performed during SR1805 at Station PS3 (coastal
347 waters) at two deoxygenated depths: 60 m and 160 m. Incubations were performed in the same
348 manner as the above anammox, denitrification, and NO₂⁻ oxidation experiments where all three
349 rates were measured in the same exetainers. Experiments consisted of eight total treatments:
350 four varying ¹⁵NO₂⁻ tracer concentrations (1.125, 5.25, 10.5, and 20.25 μM for 160 m and 0.75,
351 1.5, 3.75, and 7.5 μM for 60 m) and two ¹⁴NO₃⁻ treatments (0 or 20 μM). As above, both ³⁰N₂
352 and NO₃⁻ production via the denitrifier method (Weigand et al., 2016) were measured. In order
353 to test our hypothesis that, if dismutation is occurring, the unexplained NO₂⁻ oxidation rate (the
354 difference between the measured NO₂⁻ oxidation and the NO₂⁻ oxidation due to anammox) and
355 the denitrification rate (i.e. the ³⁰N₂ production rate) should have a 3:1 ratio, a previously
356 published anammox stoichiometry (Eq. (4) (Kuenen, 2008)) was used to calculate the NO₂⁻



357 oxidation due to anammox. The anammox rates used for this calculation are included in the
358 supplementary material (Fig. S4).

359

360 **2.7 Calculation of N loss from NH_4^+ oxidation**

361 The calculation of the maximum possible N loss from NH_4^+ oxidation via NO
362 disproportionation by ammonium oxidizing archaea (AOA) in Supplementary Table S5 was
363 carried out by dividing the measured NH_4^+ oxidation rate by two in accordance with the
364 stoichiometry of NH_4^+ oxidation and NO disproportionation proposed in a previous study (Kraft
365 et al., 2022). It should be noted that this operation represents the extreme case where all $^{15}\text{NO}_2^-$
366 produced in NH_4^+ oxidation is converted to N_2 . We acknowledge this as an unrealistic
367 assumption used to evaluate the extreme limits of the amount of total N loss attributable to NH_4^+
368 oxidation. This operation was carried out for all depths where NH_4^+ oxidation, anammox, and
369 denitrification rates were measured, irrespective of O_2 concentration.

370

371 **2.8 Redundancy analysis (RDA), Principle component analysis (PCA), and statistics**

372 All RDA, PCA, redundancy, and correlation analyses were performed with the available
373 packages in R (v4.2.1 “Funny-Looking Kid”) (R: A language and environment for statistical
374 computing). All data were first normalized around zero before calculating the Pearson’s
375 correlation coefficient. Gene abundances (nirS and amoA) used for the RDA and correlation
376 analyses were measured as previously described (Peng et al., 2015; Jayakumar et al., 2009; Tang
377 et al., 2022).

378

379 **2.9 Definition of shallow boundary and ODZ core nomenclature**



380 In the results and discussion sections, results are classified as shallow boundary or ODZ
381 core waters according to a previously published threshold (Babbin et al., 2020) where shallow
382 boundary samples have an in situ potential density < 26.4 . This method is based on a global
383 profile of OMZ waters meant to delineate shallow boundary samples as waters that are oxic or
384 may be influenced by O_2 intrusions (the surface, the oxycline, and the ODZ top) from those that
385 are not influenced by O_2 intrusions (ODZ core). It should be noted that a few samples labelled
386 as ODZ core based on the above criteria are from the deep oxycline waters below the ODZ.

Depth	σ_θ	OMZ features	O_2 intrusions?
Shallow boundary waters	< 26.4	Surface, oxycline, ODZ top	Yes
ODZ core	> 26.4	ODZ core	No

387
388 **Table 1:** Explanation of shallow boundary waters and ODZ core potential density based
389 nomenclature (Babbin et al., 2020).

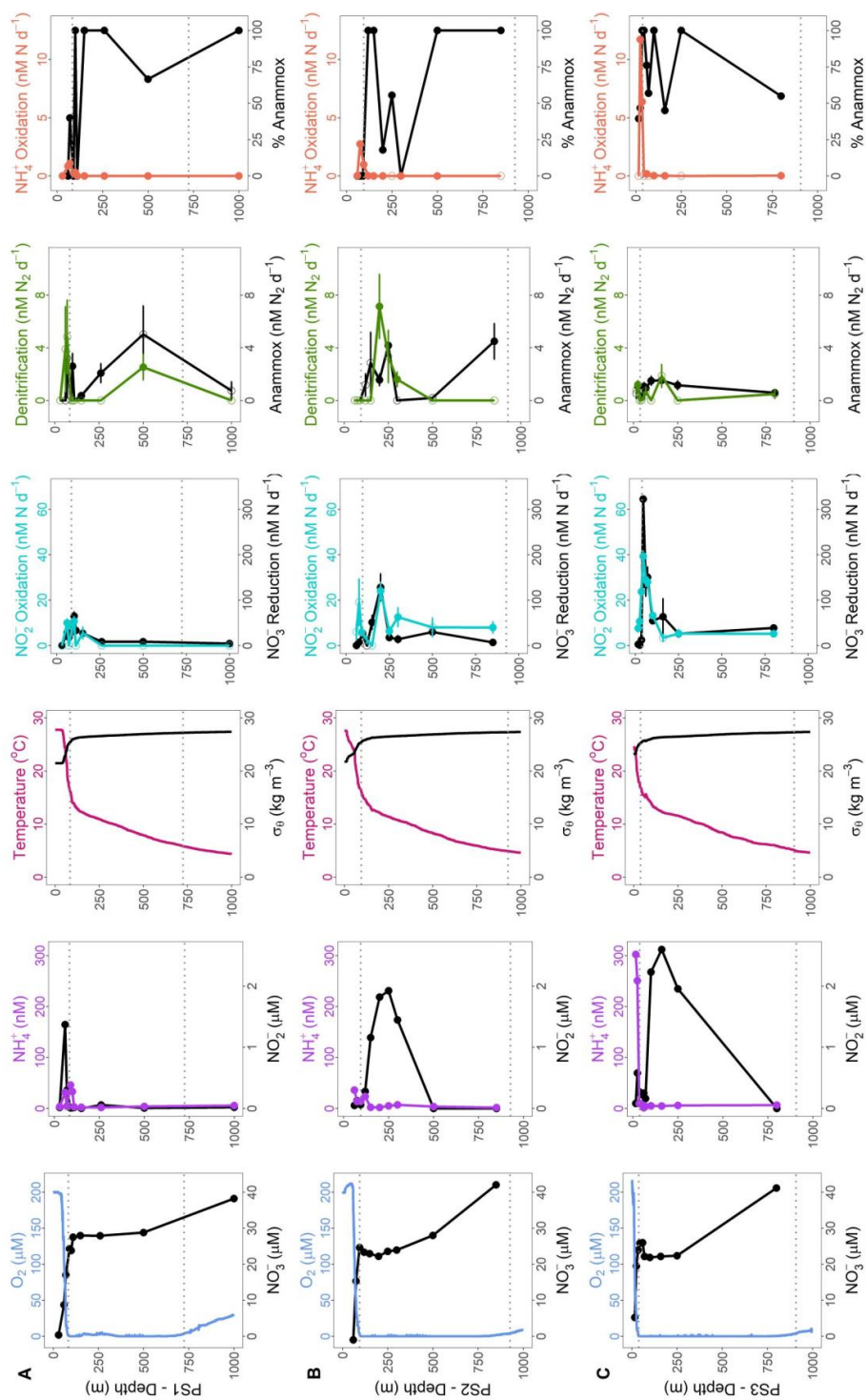
390
391 **3. Results**

392 **3.1 2018 depth profiles of all N cycling rates**

393 N cycling depth profile experiments were conducted on two cruises (SR1805 and
394 FK180624) during spring and summer 2018. These two cruises sampled stations along a
395 gradient from the edge of the OMZ region to near the coast. Physical and chemical conditions
396 varied among stations PS1, PS2, and PS3 on the SR1805 cruise (spring 2018) and across all
397 FK180624 stations (summer 2018) (Fig. 2, Fig. S1). Broadly speaking, the vertical span of the
398 ODZ increased and the top of the ODZ shoaled as distance to shore decreased. Deep SNM were
399 observed at almost all stations with the only exceptions being the furthest offshore stations,
400 stations 11 and 18 from the FK180624 cruise (Fig. S1) and station PS1 from SR1805 (Fig. 2A).
401 Peak NO_2^- values for all SNM were on the lower side of the range of previous ETNP
402 observations (Horak et al., 2016), between 1.4 – 2.6 μM .



403 Of the five N cycling processes measured on the SR1805 cruise, NO_3^- reduction rates had
404 the greatest magnitude at most depths. This trend was most pronounced within the upper ODZ,
405 where NO_3^- reduction rates peaked at station PS2, and the oxycline where NO_3^- reduction rates
406 peaked at stations PS1 and PS3 (Fig. 2). Rates of NO_2^- oxidation closely tracked NO_3^- reduction
407 in distribution; in fact, peak NO_2^- oxidation rates co-occurred with peak NO_3^- reduction rates at



408



409 **Figure 2:** SR1805 depth profiles of physical parameters and N cycling rates. **(A)** From left to
410 right, O_2 (μM) and NO_3^- (μM) respectively in blue and black, NH_4^+ (nM) and NO_2^- (μM)
411 respectively in purple and black, temperature ($^\circ\text{C}$) and σ_θ (kg m^{-3}) respectively in pink and black,
412 NO_2^- oxidation and NO_3^- reduction rates (nM N d^{-1}) respectively in cyan and black, anammox
413 and denitrification rates ($\text{nM N}_2 \text{d}^{-1}$) respectively in black and green, NH_4^+ oxidation rates (nM
414 N d^{-1}), and percent anammox respectively in coral and black for station PS1 (offshore). **(B)** As
415 above but for station PS2 (OMZ). **(C)** As above but for station PS3 (coastal). Rates that are
416 significantly different from zero are shown as filled circles, open circles signify rates not
417 significantly different from zero. Error bars are the standard error of the regression. Grey dotted
418 lines indicate upper and lower ODZ boundaries at the time of sampling.

419
420 all three SR1805 stations, reaching maxima of ~ 40 (NO_2^- oxidation) and ~ 300 (NO_3^- reduction)
421 nM N d^{-1} at PS3. However, the magnitudes of NO_2^- oxidation rates were usually lower than
422 NO_3^- reduction rates, sometimes by as much as eightfold. The third N recycling process, NH_4^+
423 oxidation, peaked at or above the oxycline, with peaks of 10 nM N d^{-1} or less. NH_4^+ oxidation
424 was consistently measured to be zero or near-zero throughout the rest of the water column.

425 Across all SR1805 and FK180624 stations, the magnitude of the N loss processes of
426 anammox and denitrification was almost always less than $10 \text{ nM N}_2 \text{d}^{-1}$, a much lower magnitude
427 than the N recycling processes of NO_3^- reduction and NO_2^- oxidation. Like NO_3^- reduction and
428 NO_2^- oxidation, the two N loss rates peaked in the upper ODZ or right at the oxycline in all three
429 SR1805 stations, although a deep peak (850 m) in anammox was observed at station PS2 (Fig.
430 2B). The same pattern was observed in the FK180624 stations with enough coverage of the
431 entire ODZ water column, stations 2, 9 (6 July sampling), and 9 (9 July sampling) (Fig. S1). The
432 relative balance between the two N loss processes as measured by percent anammox varied
433 widely across the water column but largely deviated from the expected partitioning of at most
434 29% anammox (Dalsgaard et al., 2003, 2012). A striking example of this is that 100% anammox
435 values were observed in both ODZ core and shallow boundary (see Table 1 for definitions)
436 samples at many of the SR1805 and FK180624 stations (Fig. 2, Fig. S1).

437

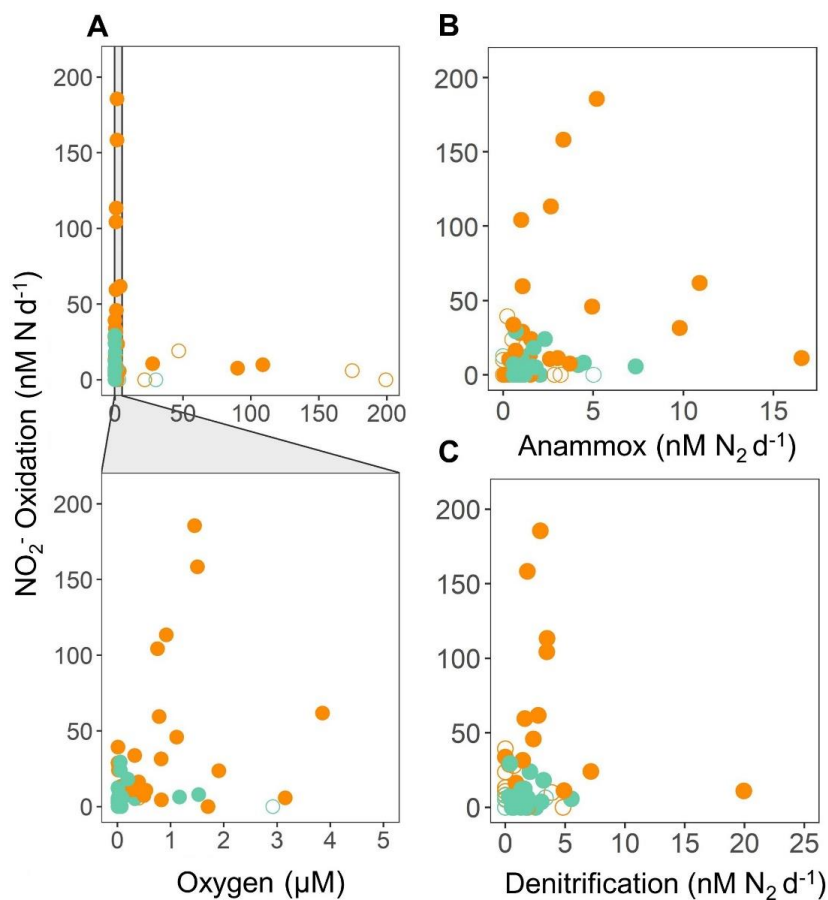


438 **3.2 Anaerobic NO₂⁻ oxidation and O₂ manipulation experiments**

439 Significant NO₂⁻ oxidation rates were detected in depth profiles across a range of suboxic
440 O₂ concentrations (1 – 5 μM) (definition from (Berg et al., 2022)) across all SR1805 stations,
441 often at the same depths and in the same vials where the obligately anaerobic processes of
442 anammox and denitrification were occurring (Fig. 2, Fig. 3A-C, Fig. S2). In order to
443 contextualize our observations, we compared our results to previously published measurements
444 from the TN278 and NBP1305 cruises performed with identical procedures (Babbin et al., 2020).
445 The highest rates were observed in shallow boundary waters across all three cruises (Fig. 3A-C,
446 Fig. S2). Since low but significant levels of O₂ can still support aerobic NO₂⁻ oxidation, a series
447 of O₂ manipulation experiments was carried out on both the SR1805 (spring) and FK180624
448 (summer) 2018 cruises (Fig. 4A-F and Fig. S3). In these experiments, where the existence of
449 functionally anoxic conditions was checked using a LUMOS O₂ optode with a detection limit of
450 0.5 nM (Lehner et al., 2015), we observed significant NO₂⁻ oxidation, as well as NO₃⁻ reduction
451 at putative concentrations as low as 1 nM. Notably, compared to previous experiments, gas
452 flushing was constant, with a refresh time of 8 min, so as to maintain O₂ levels within the
453 incubation even while organisms were respiring. Below 3 nM, O₂ is so scarce that such waters
454 are classified as functionally anoxic, i.e. O₂ cannot play biological or biogeochemical roles (Berg
455 et al., 2022). As a result, these experiments present convincing additional evidence for the
456 occurrence of NO₂⁻ oxidation up to ~100 nM N d⁻¹ at O₂ concentrations too low to support
457 aerobic metabolisms.

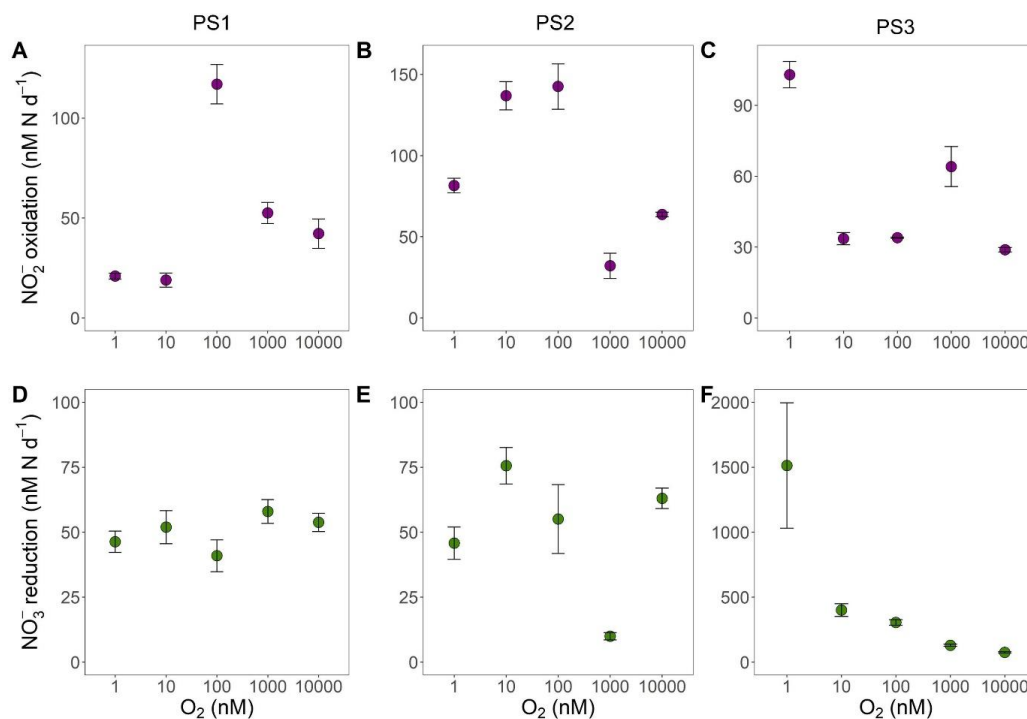
458

459



460
461

462 **Figure 3:** NO₂⁻ oxidation rates (nM N d⁻¹) from the 2018 SR1805, TN278 (ETNP 2012), and
463 NBP1305 (ETSP 2013) cruises vs. (A) O₂ concentration (μM) from shipboard CTD sensors, (B)
464 anammox rates (nM N₂ d⁻¹), and (C) denitrification rates (nM N₂ d⁻¹). In A, O₂ concentrations
465 were normalized across cruises. Rates that are significantly different from zero as assessed via a
466 Student T-test (p value < 0.05) are displayed as filled circles, while insignificant NO₂⁻ oxidation,
467 anammox, and denitrification rates are shown as open circles. Rates measured in shallow
468 boundary waters are colored orange while rates from the ODZ core and below are colored teal.
469 2012 and 2013 data are republished (Babbin et al., 2020).



470
471 **Figure 4:** Oxygen manipulation experiments that show NO₂⁻ oxidation (purple) (A-C) and NO₃⁻
472 reduction (green) (D-F) rates (nM N d⁻¹) measured across putative O₂ concentrations from 1 to
473 10,000 nM during the SR1805 cruise. Experiments were conducted with waters from the ODZ
474 top: 93 – 110m (PS1) (A, D), 113 – 130m (PS2) (B, E), and 45 – 60m (PS3) (C, F). Error bars
475 are the standard error of the regression. All rates were significantly different from zero.

476

477

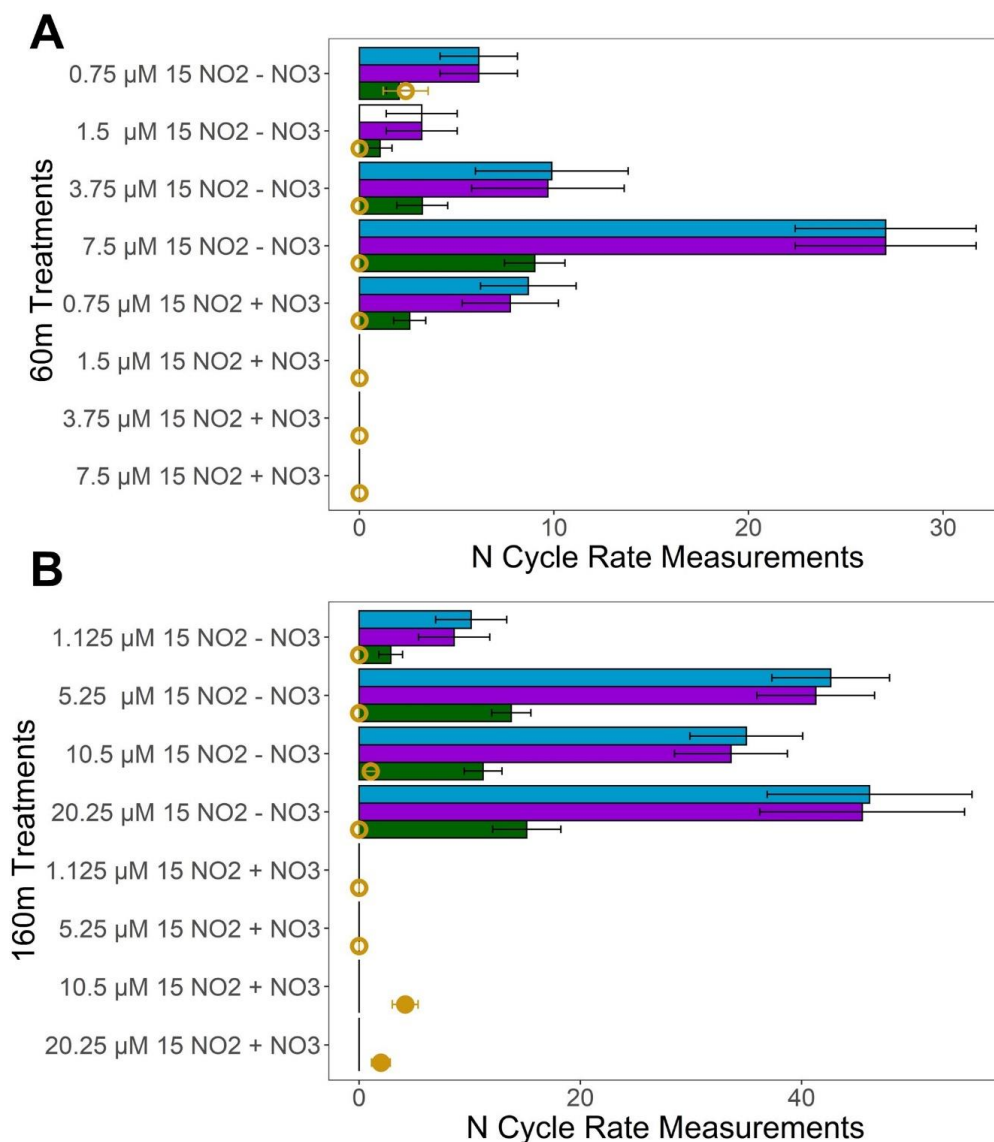
478 3.3 NO₂⁻ dismutation

479 In order to investigate the mechanism for the observed anaerobic NO₂⁻ oxidation,
480 experiments were conducted to search for evidence of NO₂⁻ dismutation. If NO₂⁻ dismutation is
481 the dominant explanation for the observed anaerobic NO₂⁻ oxidation, we hypothesized that (1)
482 adding NO₃⁻ should suppress both ³⁰N₂ and NO₃⁻ production by LeChatelier’s principle, (2)
483 increasing ¹⁵NO₂⁻ concentration should increase both denitrification (the ³⁰N₂ production rate)
484 and NO₂⁻ oxidation especially when no additional NO₃⁻ was added, and (3) that the ratio
485 between the “unexplained NO₂⁻ oxidation,” i.e., the difference between the observed NO₂⁻



486 oxidation and the NO_2^- oxidation due to anammox, and the observed denitrification ($^{30}\text{N}_2$
487 production) rate should be close to 3:1. In experiments with He-purged water from two
488 deoxygenated depths (60 and 160 m at station PS3) during the SR1805 cruise we observed that
489 adding 20 μM NO_3^- suppressed NO_2^- oxidation across nearly all pairs where NO_2^- was identical
490 and NO_3^- varied between 0 or 20 μM NO_3^- (Fig. 5). However, we did not observe a
491 simultaneous suppression of N_2 production due to the fact that the measured denitrification rate
492 was low and insignificantly different from zero in most of our 16 treatments (Fig. 5). As a result,
493 our first hypothesis yielded little evidence of dismutation.

494 Across all four 60 m 0 μM added NO_3^- treatments (Fig. 5A), adding NO_2^- did increase
495 NO_2^- oxidation; however, we did not observe an increase in denitrification. Surprisingly, across
496 the four 60 m 20 μM added NO_3^- treatments, adding NO_2^- decreased NO_2^- oxidation, the reverse
497 of our hypothesis (Fig. 5). Across all four 160 m 0 μM added NO_3^- treatments, we also observed
498 an increase in NO_2^- oxidation at higher NO_2^- concentrations but did not observe an increase in
499 the measured denitrification rate (Fig. 5B). In the four 160 m 20 μM added NO_3^- treatments,
500 NO_2^- oxidation and denitrification did not increase with NO_2^- concentration (Fig. 5B). Due to
501 the consistently low and insignificant denitrification rates our test of the NO_2^- addition
502 hypothesis also yielded little evidence for dismutation.



503

504 **Figure 5:** NO_2^- dismutation tests conducted in deoxygenated waters from 60m (A) and 160m (B)
 505 at station PS3 during the SR1805 cruise. Measured NO_2^- oxidation rates (nM N d^{-1}) are
 506 displayed in blue, unexplained NO_2^- oxidation rates, the difference between the measured NO_2^-
 507 oxidation and the NO_2^- oxidation due to anammox (nM N d^{-1}), are shown in purple. The
 508 predicted denitrification ($\text{nM } ^{30}\text{N}_2 \text{ d}^{-1}$) if all the unexplained NO_2^- oxidation was due to NO_2^-
 509 dismutation is shown in green. The measured denitrification rate ($\text{nM } ^{30}\text{N}_2 \text{ d}^{-1}$) is shown in
 510 yellow where filled circles indicate significant rates and open circles indicate rates that are not
 511 significantly different from zero. All bars filled with colors indicate significant rates (i.e. the



512 white bar for the 60 m $1.5 \mu\text{M } ^{15}\text{NO}_2^-$, $0 \mu\text{M } \text{NO}_3^-$ treatment NO_2^- oxidation rate denotes an
513 insignificant rate). Error bars are the standard error of the regression for NO_2^- oxidation, or are
514 calculated based on the rules of error propagation from the standard error of the regressions for
515 the NO_2^- oxidation and anammox rates. (+) NO_3^- treatments received $20 \mu\text{M } ^{14}\text{NO}_3^-$ additions
516 while the (-) NO_3^- treatments received no addition. Anammox rates used to calculate the
517 unexplained NO_2^- oxidation rate are shown in the supplementary material.

518
519 We were also unable to observe evidence for the ratio hypothesis due to the paucity of
520 significant denitrification ($^{30}\text{N}_2$ production) rates (Fig. 5). Since denitrification rates were
521 consistently low or insignificantly different from zero, the ratio of NO_2^- oxidation to
522 denitrification deviated from the 3:1 ratio expected if NO_2^- dismutation accounts for most of the
523 observed NO_2^- oxidation. The only slight exception to this is the 60 m treatment with $0.75 \mu\text{M}$
524 $^{15}\text{NO}_2^-$ and $0 \mu\text{M}$ added NO_3^- , the treatment closest to in situ conditions. In this treatment, the
525 measured denitrification rate, while insignificantly different from zero on the basis of the p value
526 of the regression, agrees with the predicted denitrification rate based on the 3:1 stoichiometry of
527 dismutation. While our dismutation experiments as a whole suggest that NO_2^- dismutation is not
528 a likely explanation for observed anaerobic NO_2^- oxidation, results from the 60 m $0.75 \mu\text{M}$
529 $^{15}\text{NO}_2^-$, $0 \mu\text{M } \text{NO}_3^-$ treatment provide slight justification to continue tests of this hypothesis.

530

531 **4. Discussion**

532 **4.1 Rapid $\text{NO}_2^- / \text{NO}_3^-$ cycle**

533 Depth profiles of N transformation rates obtained on the SR1805 cruise show that the
534 rates of NO_2^- oxidation and NO_3^- reduction are far greater than rates of the N loss processes of
535 anammox and denitrification, especially in shallow boundary (see Table 1 for definition) waters
536 (Fig. 2, Fig. 6A – B). In fact, when the combined N recycling pathways of NO_2^- oxidation and
537 NO_3^- reduction are compared to the total N loss, the N recycling pathways are 3.2 – 192.8 times
538 larger than the total N loss. That the minimum ratio is ~ 3 strongly emphasizes the



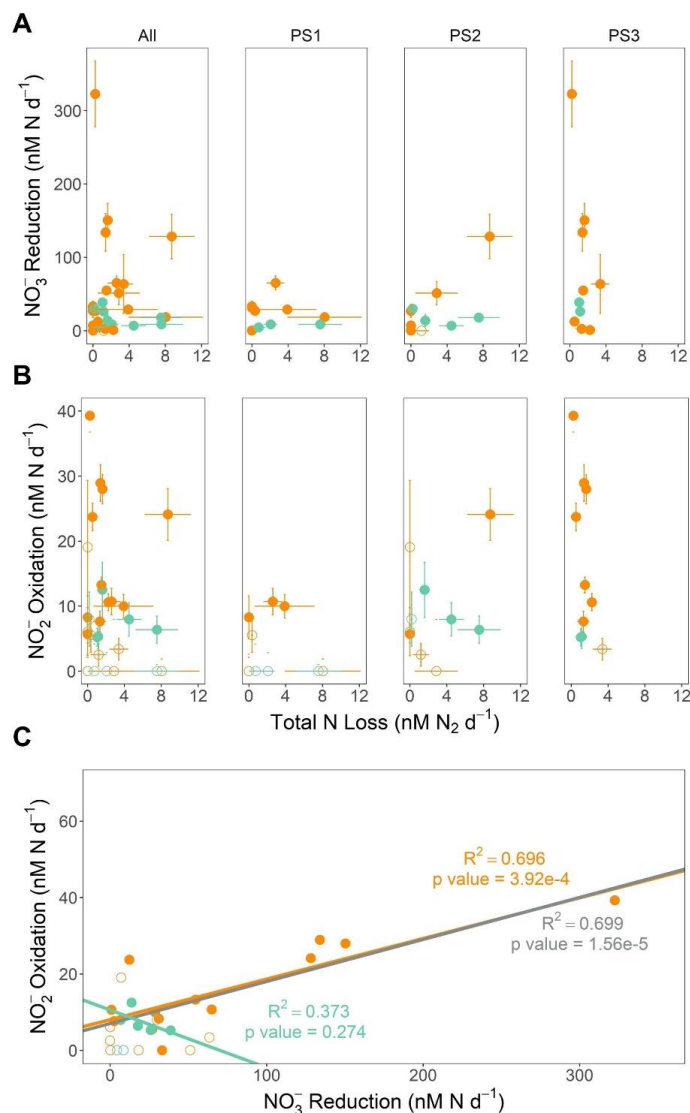
539 preponderance of NO_2^- oxidation and NO_3^- reduction above N loss processes. As expected due
540 to the lower OM concentrations offshore and as previously found in an ETSP N cycling study
541 (Kalvelage et al., 2013), NO_2^- oxidation and NO_3^- reduction generally increased from the
542 offshore station (PS1) towards the coast. We observed NO_3^- reduction rates of a similar
543 magnitude to previously reported ETSP studies (Kalvelage et al., 2013; Babbin et al., 2017), a
544 finding that generalizes the predominance of NO_3^- reduction to NO_2^- to the ETNP. Thus, our
545 work supports several recent studies (Babbin et al., 2020, 2017; Peters et al., 2016) suggesting
546 that most nitrogen within OMZ regions is continuously recycled between NO_2^- and NO_3^- by rapid
547 NO_2^- oxidation and NO_3^- reduction, especially in shallow boundary waters.

548 A previous work (Babbin et al., 2017) predicted that NO_3^- reduction should follow a
549 Martin curve (Martin et al., 1987) power law distribution across the water column due to its
550 dependence on the OM flux from shallower waters. Such a distribution was observed at stations
551 PS1 and PS3; however, NO_3^- reduction at station PS2 did not follow a classical Martin curve
552 profile since the NO_3^- production peak is well below the oxycline. An additional interesting
553 trend specific to station PS2 is that the deeper peak of NO_3^- reduction coincides with a peak in
554 complete denitrification to N_2 and a steep drop in the percent of N loss due to anammox (Fig. 2).
555 This connection is also visible in Fig. 6B which shows that NO_3^- reduction increases with total N
556 loss at station PS2.

557 These results are consistent with the idea, also supported by many recent studies (Kalvelage et
558 al., 2013; Lam and Kuypers, 2011; Lam et al., 2009; Babbin et al., 2020, 2017; Füssel et al.,
559 2011; Lam et al., 2011), that the accumulated NO_2^- in the SNM usually results from an
560 imbalance between NO_3^- reduction and other N cycling pathways. We further investigated this
561 hypothesis by constructing a net NO_2^- budget derived from the five microbial N cycling

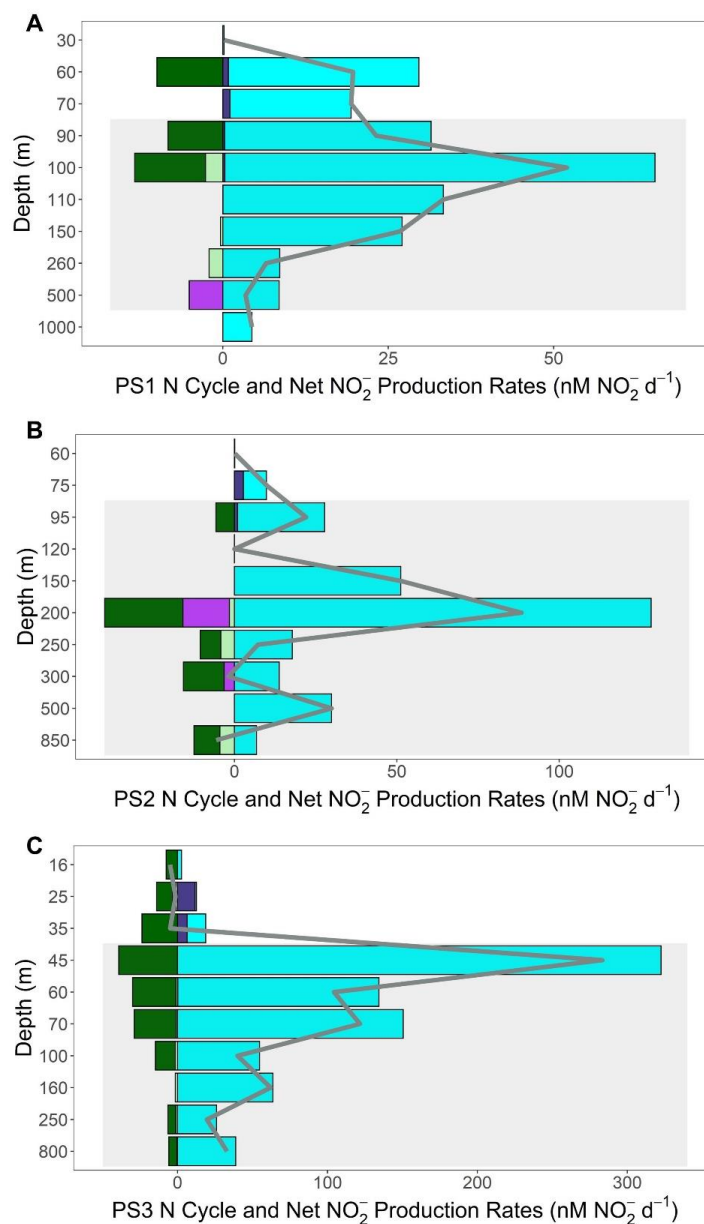


562 metabolisms measured on the SR1805 cruise (Fig. 7). Summing the depth profiles of NO_2^-
563 consumption (anammox, denitrification, and NO_2^- oxidation) and production (NH_4^+ oxidation
564 and NO_3^- reduction) pathways revealed that net depth integrated NO_2^- production across the
565 sampled OMZ water column depths is on the order of tens of millimoles of NO_2^- per square
566 meter per day at all three stations (8.19 at PS1, 14.49 at PS2, and 28.97 $\text{mmol NO}_2^- \text{ m}^{-2} \text{ d}^{-1}$ at
567 PS3). This excess NO_2^- is driven by NO_3^- reduction, which across all stations is of a much
568 greater magnitude than all other measured N cycling processes (Fig. 2 and Fig. 7). Additional
569 support that NO_3^- reduction supplies the accumulated NO_2^- in the SNM can be found by
570 comparing the net NO_2^- production rates with the measured NO_2^- concentrations along the
571 SR1805 cruise track from offshore station PS1 to coastal station PS3. As would be expected if
572 the SNM depended on NO_2^- derived from NO_3^- reduction, the peak net NO_2^- production value
573 across all depths at each station, the depth integrated NO_2^- production values for each station,
574 and the magnitude of the SNM peak NO_2^- concentrations all increase together from offshore
575 station PS1 to coastal station PS3. Importantly, we did not take into account water column
576 mixing in both vertical and horizontal directions that would carry away produced NO_2^- or NO_2^-
577 assimilation into OM, and we recommend follow up studies that include parameterizations for
578 these values in OMZ N Cycling modeling.



579

580 **Figure 6:** (A) NO₃⁻ reduction (nM N d⁻¹) vs. Total N loss (the sum of denitrification and
 581 anammox in nM N₂ d⁻¹) from the SR1805 cruise. (B) NO₂⁻ oxidation (nM N d⁻¹) vs. Total N loss
 582 from the SR1805 cruise. (C) NO₂⁻ oxidation vs. NO₃⁻ reduction. Regression lines and statistics
 583 are shown for the significant rates from shallow boundary waters only (orange), ODZ core
 584 waters only (teal), and all significant data (grey). All points from shallow boundary waters are
 585 colored orange while all points from the ODZ core or below are colored teal. Open circles
 586 indicate points where the NO₃⁻ reduction rate (A), NO₂⁻ oxidation rate (B), or in (C) either NO₃⁻
 587 reduction or NO₂⁻ oxidation rate is not significantly different from zero while filled circles
 588 indicates rates significantly different from zero.



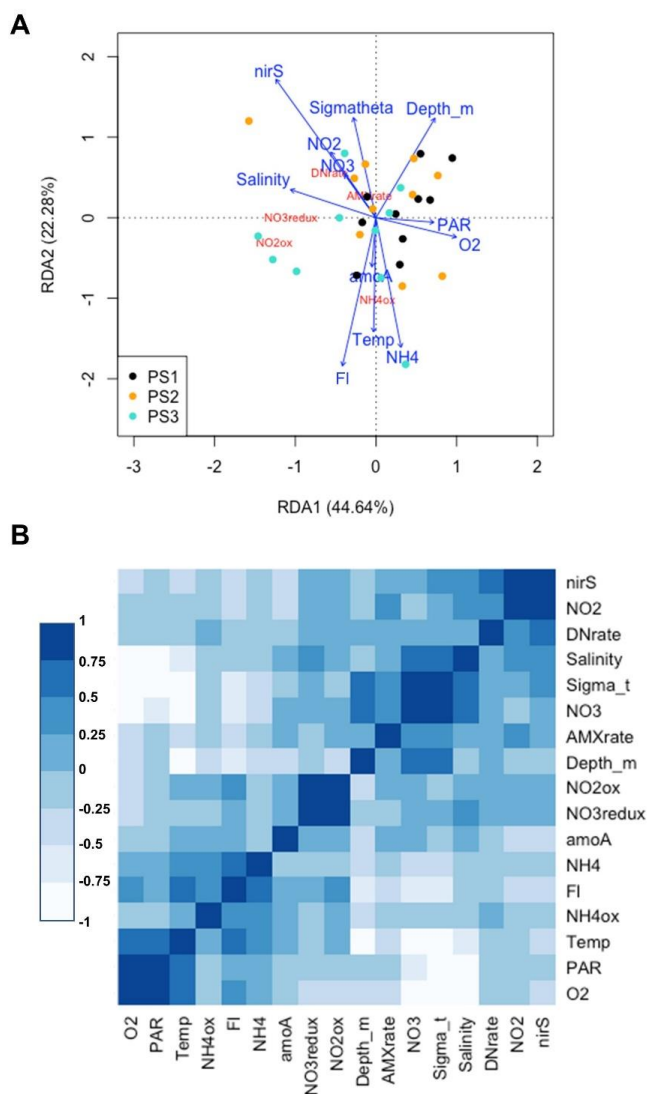
589
590

591 **Figure 7:** NO_2^- budget profiles from the SR1805 cruise. Plots are a combination of the NO_2^-
592 production pathways of NO_3^- reduction (cyan), NH_4^+ oxidation (dark purple) and the NO_2^-
593 consumption pathways of anammox (light green), denitrification (bright purple), and NO_2^-
594 oxidation (dark green). Consumption pathways are reported as negative numbers. All rates are
595 reported in $\text{nM NO}_2^- \text{d}^{-1}$. The net NO_2^- production or consumption rate ($\text{nM NO}_2^- \text{d}^{-1}$) is
596 represented as a grey line for each depth. Grey boxes indicate the completely deoxygenated
597 ODZ region at each station at the time of sampling. (A) PS1, (B) PS2, and (C) PS3.



598 **4.2 NO₂⁻ oxidation – distribution and magnitude in comparison to previous studies**

599 The high rates of observed NO₃⁻ reduction provide sufficient NO₂⁻ to support NO₂⁻
600 oxidation both in the oxycline and in the ODZ, as previously proposed (Anderson et al., 1982),
601 Our observations also further confirm isotopic studies that suggested high NO₂⁻ oxidation rates
602 because rapid re-oxidation of NO₂⁻ back to NO₃⁻ was necessary to achieve isotopic mass balance
603 (Buchwald et al., 2015; Casciotti et al., 2013; Granger and Wankel, 2016). Our results also align
604 with previous experimental observations of high NO₂⁻ oxidation rates (Kalvelage et al., 2013;
605 Babbin et al., 2020; Lipschultz et al., 1990). Support for a closely connected rapid cycle
606 between the two processes can be seen in the strong correlation between NO₂⁻ oxidation and
607 NO₃⁻ reduction observed in all SR1805 cruise samples, especially those from shallow boundary
608 waters (Fig. 6C, Fig. 8). Similarly to some previous ETSP papers (Babbin et al., 2017, 2020;
609 Frey et al., 2020) and two ETNP studies (Peng et al., 2015; Sun et al., 2017) we observed that
610 rates of NO₂⁻ oxidation, like rates of NO₃⁻ reduction, peaked in the oxycline or in the ODZ top
611 (Fig. 2) and then declined throughout the ODZ. Unlike some stations in these studies (Babbin et
612 al., 2020, 2017) we did not observe a second peak in NO₂⁻ oxidation near the deep oxycline. In
613 addition to observing a similar distribution, we also observed that NO₂⁻ oxidation occurs at a
614 similar magnitude to some stations in previous ETSP studies (Babbin et al., 2020, 2017; Peng et
615 al., 2016) and ETNP (Peng et al., 2015), although our highest rates (25 – 40 nM N d⁻¹) were
616 much lower than the peaks measured at other stations in most of these reports (Babbin et al.,
617 2020; Peng et al., 2015, 2016), which reached as high as ~600 nM N d⁻¹ (Peng et al., 2015;
618 Lipschultz et al., 1990).



619

Figure 8: (A) Redundancy analysis of all environmental variables and microbial rates measured on the SR1805 cruise. Points are color-coded by station, black (PS1), yellow (PS2), and cyan (PS3). Variables names and arrows are color coded so that environmental variables are blue and rate measurements are red. (B) Correlation analysis for all environmental variables and microbial N cycle rates from the SR1805 cruise. More positive correlations are shaded to become bluer as significance grows while negative correlations are shaded to become whiter as significance grows. Abbreviations used are as follows: O2 (oxygen concentration normalized across different sensors), PAR (photosynthetically active radiation normalized across sensors), NH4ox (NH₄⁺ oxidation rate), FI (chlorophyll fluorescence normalized across different sensors), NH4 (NH₄⁺ concentration), amoA (*amoA* abundance), NO₃-redux (NO₃⁻ reduction rate), NO2ox



630 (NO_2^- oxidation rate), AMXrate (anammox rate), NO_3^- (NO_3^- concentration), DNrate
631 (denitrification rate), NO_2 (NO_2^- concentration), and nirS (*nirS* abundance).

632

633

634 **4.3 NO_2^- oxidation – can it occur anaerobically?**

635 NO_2^- oxidation depth profiles (Figs. 2, 3) and O_2 manipulation experiments (Fig. 4)

636 provide further evidence that NO_2^- oxidation can occur under functionally anoxic conditions.

637 While O_2 was not directly measured in the depth profile experiments, several factors argue that

638 the NO_2^- oxidation observed in these incubations may be O_2 independent. As argued previously

639 (Babbin et al., 2020):

640 (1) The pre-incubation He purging step in our method removes more than 99% of the N_2 present

641 in exetainers (Babbin et al., 2020). If it is assumed that O_2 is removed at identical efficiency, a

642 reasonable proposition since O_2 equilibrates faster than N_2 (Wanninkhof, 1992), the introduction

643 during sample processing of as much as $1 \mu\text{M}$ O_2 would result in a ~ 10 nM contamination. As a

644 result, if NO_2^- oxidation is observed in samples from the deoxygenated ODZ core, contamination

645 during sampling would be kept very small by our purging step.

646 (2) Linear timecourses across all timepoints were observed in some of our experiments,

647 including many from deoxygenated depths at station PS3 (Supplemental Figs. S7-9). If NO_2^-

648 oxidation depended on O_2 , an initial acceleration (due to O_2 contamination that sparked NO_2^-

649 oxidation) or later steep drop (due to the exhaustion of O_2 by aerobic NOB) in NO_2^- oxidation

650 would be expected, not a consistent linear slope.

651 (3) Metagenomic evidence has revealed distinct NOB communities in oxic surface waters, the

652 oxycline and ODZ top, and the ODZ core in OMZ regions (Sun et al., 2019). In addition we

653 observed decreasing NO_2^- oxidation rates with increasing in situ O_2 in the SR1805 incubations as

654 well as the TN278 and NBP1305 incubations (Fig. 3A). These observations are consistent with



655 the hypothesis that aerobic NOB from oxic depths are ill-equipped to oxidize NO_2^- in
656 deoxygenated conditions but that the unique MAGs recently identified in draft genomes from the
657 ODZ top and core (Sun et al., 2019), are adapted to perform anaerobic NO_2^- oxidation.

658 (4) We observed NO_2^- oxidation at the same depths and often in the same incubation vessels as
659 the obligately anaerobic processes of anammox and denitrification (Fig. 2, Fig. 3B-C). Our
660 observations are consistent with several previous observations that these processes occur at the
661 same depths (Babbin et al., 2020; Sun et al., 2021).

662 (5) Through plotting O_2 concentrations against the ratio between NO_3^- reduction and NO_2^-
663 oxidation at all SR1805 depths with significant, positive NO_2^- oxidation rates we observed that
664 the known anaerobic process of NO_3^- reduction and NO_2^- oxidation did not exhibit differential
665 regulation by O_2 as would be expected if NO_2^- oxidation was an obligately aerobic process (Fig.
666 S5).

667 Previous studies have shown that O_2 additions to purged incubations of ODZ waters
668 inhibit NO_2^- oxidation (Sun et al., 2017, 2021) and that NO_2^- oxidation can occur in the absence
669 of O_2 consumption (Sun et al., 2021). However, another kinetics study has reported O_2
670 stimulation of NO_2^- oxidation in OMZ waters (Bristow et al., 2016) and concluded that NO_2^-
671 oxidation is fundamentally an aerobic process. This apparent contradiction might be explained
672 by several details in the experimental process of that study:

673 (1) The study site is at the farthest edge of the ETSP OMZ in a location that is only anoxic in the
674 austral summer.

675 (2) The cruise was conducted as austral summer turned to fall (March 20 – 26th), a period where
676 O_2 intrusions would be more likely.



677 (3) O₂ data from the study's cruise (Tiano et al., 2014) show that the depths from which NO₂⁻
678 oxidation O₂ kinetics samples were sourced experienced O₂ concentrations of 2 μM (50 m), 10
679 μM (40 m), and > 60 μM (30m) either during sampling or a few days prior to sampling.
680 As a result, we argue that the observed stimulation of NO₂⁻ oxidation by O₂ (Bristow et al., 2016)
681 occurred not because all OMZ NOB are aerobic NO₂⁻ oxidizers, but instead because the location,
682 season, and levels of O₂ of the sampled station selected for aerobic NOB in the source water for
683 the purged incubations. Thus, as suggested by (Sun et al., 2017, 2021), different NOB
684 populations with different historical exposures to O₂ and adaptations likely respond differently to
685 O₂ manipulations.

686 Here we built on the above previous tests of anaerobic NO₂⁻ oxidation by conducting a
687 series of incubations across an O₂ gradient from 1 nM to 10 μM. Site waters for these
688 incubations were drawn from the ODZ top at each SR1805 station. We did not observe a clear
689 inhibitory or stimulatory response of NO₂⁻ oxidation to O₂ within the SR1805 or FK180624
690 stations, however, this lack of a clear response is in itself a revealing result - a lack of consistent
691 stimulation by O₂ implies at least some anaerobic NOB were present. In addition, we
692 consistently observed significant NO₂⁻ oxidation at all putative O₂ concentrations, including 1
693 nM, a functionally anoxic oxygen concentration, i.e., one unable to support aerobic metabolisms
694 (Berg et al., 2022). Since the initial O₂ was supplied by a mass flow controller and subsequently
695 checked via a very sensitive O₂ sensor for all incubations, these results provide additional
696 evidence that truly anaerobic NO₂⁻ oxidation can occur.

697 These O₂ manipulation experiments also provided an opportunity to investigate the
698 response of NO₃⁻ reduction to O₂. The only clear intra-station pattern that emerged from these
699 experiments was that at station PS3, NO₃⁻ reduction displayed possible inhibition by O₂, as



700 would be expected. Due to the low number of data points in our data set we did not attempt a
701 kinetics fitting for this data. Interestingly, the gap observed in depth profile experiments
702 between the magnitudes of the NO_3^- reduction and NO_2^- oxidation rates was not observed in the
703 O_2 manipulations across many O_2 concentrations at stations PS1 and PS2. At station PS3 a large
704 gap in the magnitudes of these processes as well as the highest overall NO_3^- reduction rates were
705 observed, as in the depth profile experiments (Fig. 4, 7). A few of the FK180624 data points also
706 exhibited NO_3^- reduction rates that were elevated far above NO_2^- oxidation (Fig. S3). These
707 results confirm the importance of NO_3^- reduction for the rapid recycling cycle as well as the
708 source of NO_2^- for the SNM.

709

710 **4.4 NO_2^- dismutation**

711 In the absence of O_2 , NO_2^- oxidation would require another oxidant. Many candidate
712 oxidants have been suggested. For example, iodate (IO_3^-), an abundant marine species with
713 global average marine concentrations of $\sim 0.5 \mu\text{M}$ (Nozaki, 1997; Lam and Kuypers, 2011), has
714 been proposed and shown to stimulate NO_2^- oxidation (Babbin et al., 2017). However, since
715 IO_3^- is usually absent within the ODZ core (Moriyasu et al., 2020), its low concentration makes
716 IO_3^- mediated anaerobic NO_2^- oxidation unlikely (Babbin et al., 2020). NO_2^- oxidation via Mn^{4+}
717 or Fe^{3+} is thermodynamically feasible, but only at low pH (< 6) (Luther, 2010; Luther and Popp,
718 2002). This pH constraint, combined with the fact that concentrations of these ions are on the
719 order of a few nM in OMZs (Kondo and Moffett, 2015; Vedamati et al., 2015), makes these
720 mechanisms unrealistic for the ODZ core. Another proposed mechanism is that the observed
721 NO_2^- oxidation is due to anammox, which if true should result in an observed NO_2^- oxidation to
722 anammox ratio of 0.16 – 0.3 (Kuenen, 2008; Strous et al., 1998; Oshiki et al., 2016). Instead, the



723 observed ratio is sometimes more than 10x this range and NO_2^- oxidation is rarely observed to be
724 less than anammox (Kalvelage et al., 2013; Babbin et al., 2020; Sun et al., 2021).

725 Another alternative hypothesis is based on the reversibility of the nitrite oxidoreductase
726 (NXR) enzyme. Since this enzyme has been suggested to both oxidize NO_2^- and reduce NO_3^-
727 (Kemeny et al., 2016; Koch et al., 2015; Wunderlich et al., 2013), NO_3^- reduction by NXR could
728 over time enrich the ^{15}N - NO_3^- pool since lighter $^{14}\text{NO}_3^-$ would be favored (Casciotti, 2009).
729 Even in $^{15}\text{NO}_2^-$ tracer experiments, in which the NO_2^- pool is highly labeled, this reversibility at
730 the enzyme site could lead to an apparent transfer of ^{15}N from the NO_2^- to the NO_3^- pool if NXR
731 mediated NO_3^- reduction was occurring. This hypothesis is supported by observations of NO_3^-
732 reduction under low O_2 in cultures from the NOB genera *Nitrobacter* (Freitag et al., 1987; Bock
733 et al., 1990), *Nitrospira* (Koch et al., 2015), and in pure cultures of *Nitrococcus mobilis* (Füssel
734 et al., 2017). In addition, a recent study presented natural abundance isotopic evidence in pure
735 *Nitrococcus mobilis* cultures consistent with this mechanism (Buchwald and Wankel, 2022).

736 However, NXR reversibility has not been demonstrated for the abundant (Füssel et al.,
737 2011; Mincer et al., 2007) and sometimes predominant (Beman et al., 2013) OMZ NOB genera
738 *Nitrospina*. Furthermore, the sole source of the isotopic evidence for the enzyme reversibility
739 hypothesis, *Nitrococcus mobilis*, has a cytoplasm facing NXR substrate binding domain
740 (Buchwald and Wankel, 2022), a feature found to have an established evolutionary relationship
741 to NAR (the known NO_3^- reductase enzyme family) in other *Nitrobacter* studies (Starkenburg et
742 al., 2008; Kirstein and Bock, 1993). The NXR substrate binding domains in *Nitrospina* are
743 oriented towards the periplasm and are not evolutionarily related to enzymes for NO_3^- reduction
744 (Buchwald and Wankel, 2022; Sun et al., 2019). Due to these structural and phylogenetic
745 differences among NOB NXR, it is possible that the *Nitrospina* NXR may be unable to perform



746 NO_3^- reduction as easily as other NOB genera. For all these reasons, it is not yet clear if the
747 enzyme reversibility hypothesis can explain all NO_2^- oxidation measured under low O_2
748 conditions and other hypotheses should continue to be explored.

749 As a result of the above proposals' shortcomings, this paper focused on the remaining,
750 most plausible hypothesis: NO_2^- dismutation. Our tests for dismutation rested on three
751 hypotheses: (1) that NO_3^- additions would inhibit both NO_2^- oxidation and $^{30}\text{N}_2$ production by
752 LeChatelier's principle, (2) that increasing $^{15}\text{NO}_2^-$ should energetically favor dismutation,
753 especially in treatments with no additional NO_3^- , and (3) that the ratio of non-anammox
754 mediated NO_2^- oxidation to denitrification ($^{30}\text{N}_2$ production) should be close to 3:1 if NO_2^-
755 dismutation explains most of the observed NO_2^- oxidation. We observed repeated inhibition of
756 NO_2^- oxidation by NO_3^- but no inhibition of $^{30}\text{N}_2$ production due to the fact that denitrification
757 was consistently low and insignificantly different from zero across all treatments. In treatments
758 with 0 μM added NO_3^- , increasing NO_2^- generally increased NO_2^- oxidation, but not
759 denitrification. In addition, the ratio of anammox corrected NO_2^- oxidation to observed
760 denitrification deviated from dismutation's 3:1 stoichiometry in almost all treatments. However,
761 we did observe simultaneous inhibition of N_2 and NO_3^- production as well as good agreement
762 between the anammox corrected NO_2^- oxidation / denitrification ratio to the NO_2^- dismutation
763 stoichiometry in one treatment - the treatment most similar to in situ conditions (60m, 0.75 μM
764 $^{15}\text{NO}_2^-$, 0 μM NO_3^-). As a result, while our results show little evidence for dismutation overall,
765 we recommend additional experiments at tracer levels similar to 0.75 μM $^{15}\text{NO}_2^-$ to further test
766 for NO_2^- dismutation.

767

768 **4.5 Relative balance of anammox and denitrification**

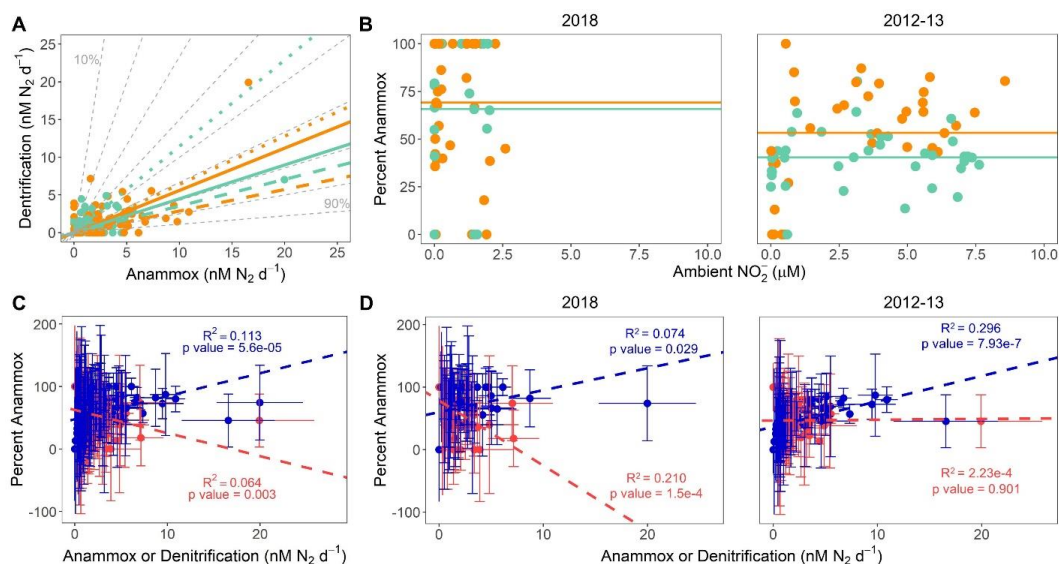


769 **4.5.1 Are results consistent with past observations of slow, low, and steady anammox**
770 **elevated above the predicted maximum of 29% of total N loss?**

771 According to predictions based on the composition of average marine OM (Dalsgaard et
772 al., 2003, 2012) anammox should account for at most 29% of the total N loss flux in OMZ
773 regions. To test this hypothesis under a variety of conditions, regressions of denitrification vs.
774 anammox rates were calculated for all samples from the SR1805, FK180624, TN278, and
775 NBP1305 cruises. In order to compare our new data to a previous study (Babbin et al., 2020),
776 which observed variations in the ratio of anammox and denitrification between samples from the
777 ODZ top or above ($\sigma_{\theta} < 26.4$, “shallow boundary waters,” (Babbin et al., 2020)) and samples
778 from the deoxygenated ODZ core or below ($\sigma_{\theta} > 26.4$, “ODZ core,” (Babbin et al., 2020)),
779 regressions for all data (ODZ core), all data (shallow boundary), 2018 only (ODZ core), 2018
780 only (shallow boundary), 2012-13 (TN278, and NBP1305) only (ODZ core), and 2012-13 only
781 (shallow boundary) were calculated (Table S4). All regressions deviated from the predicted 29%
782 maximum anammox contour, although the regression from the 2012-13 cruises’ ODZ core
783 samples was closest to the 30% anammox contour (Fig. 9A). We observed large differences in
784 the percent anammox contours near 2012-13 and 2018 regressions. ODZ core samples from
785 2012-13 regressed onto a line between the 40 and 50% anammox contours while ODZ core
786 samples from 2018 regressed onto a line between the 70% and 80% anammox contours.
787 Differences in contouring were smaller for the shallow boundary samples, although the 2018
788 samples still regressed to a higher contour (just under 80%) than the 2013-13 samples (60%)
789 (Fig. 9A). Our observations that all year and density based regressions fell within contours well
790 above the theoretical prediction (Fig. 9A) and that anammox accounted for as much as 100% of
791 the total N loss at many depths in 2018 samples (Fig. 2, Fig. 9B) is consistent with the many



792 previous studies that observed anammox as the predominant OMZ N loss pathway (Lam et al.,
 793 2009; Thamdrup et al., 2006; Kuypers et al., 2005; Hamersley et al., 2007; Jensen et al., 2011).
 794 Our new 2018 results do not contradict the idea (Dalsgaard et al., 2012) that anammox is
 795 often measured to be the bulk of total N loss but that large, episodic occurrences of denitrification
 796 can dwarf the consistent albeit low anammox contribution to total N loss. Under this view, these
 797 eruptions in denitrification return the *time integrated* balance of anammox and denitrification to
 798 its expected 29 and 71% values. In this scenario, our cruises' sampling, like many but not all
 799 others, did not coincide with episodic high rates of denitrification.



800

801 **Figure 9:** (A) All 2012, 2013, and 2018 denitrification and anammox rates ($\text{nM N}_2 \text{d}^{-1}$), color-
 802 coded by σ_θ . ODZ core samples and lines are teal ($\sigma_\theta > 26.4$) while shallow boundary samples
 803 and lines are orange ($\sigma_\theta < 26.4$). Solid, dashed, and dotted lines respectively show regressions
 804 for all data, 2018 only, and 2012-13 data only. Dashed grey lines depict contours for percent
 805 anammox values. See Supplementary Table S4 for regression statistics. (B) Percent anammox
 806 vs. ambient NO_2^- for 2018 samples (left) and republished 2012 and 2013 samples (Babbin et al.,
 807 2020) (right). Points are colored according to the same scheme as panel A. Lines show the
 808 average percent anammox values in shallow boundary waters (orange) and the deoxygenated
 809 ODZ core (teal). (C) Percent anammox vs. all anammox (blue) and all denitrification (red) rates
 810 ($\text{nM N}_2 \text{d}^{-1}$). Regression lines shown for % AMX vs. anammox and denitrification rates follow



811 the same color scheme as the data points. Error bars represent the standard error of the
812 regression. **(D)** Percent anammox vs. anammox (blue) and denitrification (red) rates ($\text{nM N}_2 \text{ d}^{-1}$)
813 for 2018 only (left) and 2012-13 (right). Points and regression lines follow the same color
814 scheme as in panel C. Data shown in the 2012-13 only panel are republished (Babbin et al.,
815 2020).

816

817

818 **4.5.2 Do results support a connection between rapid NO_3^- reduction and elevated**

819 **anammox?**

820 Our 2018 results question the previously proposed view (Babbin et al., 2020) that rapid
821 NO_3^- reduction produces NH_4^+ that in turn elevates anammox in oxycline and upper ODZ
822 waters. While our data (Fig. 2) did find high rates of NO_3^- reduction in shallow boundary
823 waters, the 2018 N loss data do not show elevated shallow boundary (as compared to ODZ core)
824 percent anammox values as would be expected if high NO_3^- reduction were fueling elevated
825 anammox in the oxycline and ODZ top. This difference between our 2018 data and some
826 previous data (Babbin et al., 2020) in support of a connection between rapid NO_3^- reduction and
827 elevated anammox in the oxycline and ODZ top can be seen through a comparison of shallow
828 boundary ($\sigma_\theta < 26.4$ (Babbin et al., 2020)) and ODZ core ($\sigma_\theta > 26.4$ (Babbin et al., 2020)) percent
829 anammox values in the 2018 SR1805 and FK180624 cruises against the 2012-13 TN278 and
830 NBP1305 cruises (Fig. 9B). 2012-13 samples showed a clear partitioning between the ODZ core
831 and shallow boundary waters in terms of percent anammox values. In 2012-13, as would be
832 expected if high oxycline and ODZ top NO_3^- reduction were supplying NH_4^+ to anammox,
833 shallow boundary samples have a higher average percent anammox value than ODZ core
834 samples (Fig. 9B). In 2018, this partitioning was not present - the difference between the
835 average percent anammox values in ODZ core and shallow boundary samples was much smaller
836 (Fig. 9B). Interestingly, the total number of samples found to be 100% anammox also sharply
837 diverged between 2012-13 and 2018. In the 2012-13 samples, only one shallow boundary



838 sample was found to be 100% anammox. In 2018, many samples from both shallow boundary
839 waters and the ODZ core were 100% anammox (Fig. 9B, Fig. S6).

840 These observed differences in the partitioning of anammox and denitrification between
841 shallow boundary waters and the ODZ core across different years and places do not support the
842 view that NH_4^+ from rapid NO_3^- reduction of oxycline and ODZ top OM always elevates
843 anammox rates. Instead, they suggest that other factors play an important role in setting the
844 balance of anammox and denitrification. Interestingly, NO_2^- concentrations spanned a much
845 narrower range in the two 2018 SR1805 and FK180624 cruises than the 2012-13 TN278 and
846 NBP1305 cruises (Fig. 9B), a clue that the biogeochemical environment of the OMZ is subject to
847 interannual variability. Observed differences in environmental variables like NO_2^- and percent
848 anammox partitioning between 2012, 2013, and 2018 suggest that the partitioning of total N loss
849 must depend on additional yet to be identified environmental or biological interactions.

850

851 **4.5.3 Correlations of percent anammox values to anammox and denitrification rates -** 852 **comparison to previous literature**

853 In order to re-examine the result (Babbin et al., 2020) that enhanced fractions of
854 anammox are correlated to greater anammox rates and not lower denitrification (Fig. 9D right),
855 we created percent anammox vs. anammox and denitrification regressions with the 2018 SR1805
856 and FK180624 data. In 2018, unlike in 2012-13 (Babbin et al., 2020), we observed significant
857 relationships between percent anammox values and both the anammox and denitrification rates
858 (Fig. 9D left). Regressions for the 2012-13 data showed that increases in % anammox values are
859 correlated only to increases in anammox values, not decreases in denitrification (Babbin et al.,
860 2020) (Fig. 9D right). The 2018 regressions, on the other hand, indicate that increases in %



861 anammox are correlated with both increasing anammox and decreasing denitrification rates. The
862 influence of this difference in the 2018 samples can be seen in regressions of % anammox
863 against anammox and denitrification from all three cruises where a similar pattern to the 2018
864 data is observed (Fig. 9C). As above, this indicates a clear difference in the partitioning of
865 anammox and denitrification between the 2018 SR1805 and FK180624 ETNP cruises and the
866 2012-13 TN278 and NBP1305 cruises to the ETNP and ETSP. Despite the significance of the
867 relationships, the low R^2 values indicate that these relationships do not explain most of the
868 variation in the anammox to denitrification ratio. As above, the causal mechanisms behind this
869 variability remains to be elucidated.

870

871 **4.5.4 Caveats about measurements of anammox and denitrification rates**

872 One important caveat to some of the above conclusions in section 4.5 is that the detection
873 limits for anammox and denitrification rates are not identical. It is easier to detect anammox for
874 a variety of reasons. For example, anammox from a $^{15}\text{NH}_4^+$ tracer is more easily detected due to
875 low background NH_4^+ across most of the OMZ. Anammox from the $^{15}\text{NO}_2^-$ tracer is more
876 detectable due to its reliance on incorporation of only a single ^{15}N atom into the $^{29}\text{N}_2$ product.
877 Denitrification, on the other hand, is more difficult to detect because of higher background NO_2^-
878 concentrations and because definitive denitrification requires the rarer combination of two
879 $^{15}\text{NO}_2^-$ molecules (Babbin et al., 2017). We suspect that denitrification's higher detection limit
880 may have played a role in our observations of denitrification rates in the 2012, 2013, and 2018
881 cruises where, for example, significant denitrification rates were only detected at four of the
882 thirty depths sampled during SR1805 (Supplementary Table S3). As a result, while the
883 comparisons made above are helpful to examine differences in N biogeochemistry across years



884 and stations, the true biogeochemical role of denitrification is likely greater than our tracer
885 experiments suggest.

886

887 **4.6 Possibility of N loss via AOA and other N cycling processes**

888 A recent paper (Kraft et al., 2022) reported that dense cultures of the ammonium
889 oxidizing archaea (AOA) *Nitrosopumilus maritimus* can support the O₂ dependent process of
890 NH₄⁺ oxidation in deoxygenated waters via NO disproportionation to O₂ and N₂. This
891 mechanism would be a third N loss process that, if occurring in OMZs, would be measured as
892 anammox or denitrification. In order to investigate the possible significance of this N loss
893 pathway in ODZ waters, we calculated the maximum possible N loss from NH₄⁺ oxidation – the
894 N loss that would result if all of the ¹⁵N-NO₂⁻ produced in our NH₄⁺ oxidation experiments was
895 converted into N₂ via the proposed NO disproportionation reaction. These maximum NH₄⁺
896 oxidation derived N loss rates were a small fraction of the total N loss rates at most depths
897 (Supplementary Table S5). As a result, even these unrealistically high estimates of N₂
898 production from AOA do not suggest that AOA are significant agents for fixed N loss. The
899 depths where this was not the case are all either oxic or upper oxycline depths where NH₄⁺
900 oxidation rates peak and do not require NO disproportionation to supply O₂, or depths where
901 equally low NH₄⁺ oxidation, anammox, and denitrification rates would allow a higher percentage
902 of the total N loss to be due to NH₄⁺ oxidation. As a result, our calculation argues that N loss
903 derived from NH₄⁺ oxidation is not a significant N loss flux in ODZs. Thus, we argue that our
904 conclusions regarding the relative balance of anammox and denitrification, as well as the
905 relationship of these two N loss processes to other parts of the N cycle, do not need to be revised
906 to account for N loss via NO disproportionation in AOA.



907 We note that an additional N recycling pathway, dissimilatory nitrate/nitrite reduction to
908 ammonium (DNRA) can occur under low O₂ conditions similar to those preferred by anammox
909 and denitrification. While some OMZ studies have found rates and *nrfA* abundances comparable
910 to anammox, denitrification, and NH₄⁺ oxidation rates and marker gene abundances (Lam et al.,
911 2009; Jensen et al., 2011), DNRA is best described as an extremely variable process. Other past
912 OMZ studies have often found negligible rates (De Brabandere et al., 2014; Kalvelage et al.,
913 2013; Füssel et al., 2011) and little genetic evidence for DNRA (Kalvelage et al., 2013). Due to
914 this variability we chose to focus this study on what are arguably the most consistently relevant
915 rates for OMZ N biogeochemistry.

916

917 **5 Conclusions**

918 Nitrogen is an essential component of life and as a result, its availability can function as a
919 cap on biological productivity in many marine ecosystems. Since all the ocean is linked through
920 an intricate web of currents that span the globe, the N biogeochemistry of small regions can
921 affect the biogeochemistry of the rest of the ocean. Although OMZs account for just 0.1 - 1% of
922 the ocean's total volume (Lam and Kuypers, 2011; Codispoti and Richards, 1976; Naqvi, 1987;
923 Bange et al., 2000; Codispoti et al., 2005) they account for 20-40% of all total marine N loss
924 (Brandes and Devol, 2002; Codispoti, 2007; Gruber, 2004). As a result, developing an
925 understanding of N cycling within OMZs is critical for comprehending the total marine N
926 budget. Here we presented measurements from the ETNP OMZ of five microbial N cycling
927 metabolisms, all of which have NO₂⁻ as a product, reactant, or intermediate. Understanding the
928 magnitudes of these rates is key to determining the OMZ inventory of N species as well as an
929 important piece of understanding the marine N budget.



930 Our results add to the growing evidence that the N recycling process of NO_3^- reduction is
931 the largest OMZ N flux followed by the recycling process of NO_2^- oxidation back to NO_3^- .
932 These two processes peaked in the oxycline or ODZ top and were usually much greater than the
933 two N loss processes of anammox and denitrification, a departure from the established view that
934 understanding N loss processes alone is the key to understanding OMZ biogeochemistry. We
935 also add further evidence to the body of literature that supports the occurrence of anaerobic NO_2^-
936 oxidation in OMZ regions, most strikingly through a series of O_2 manipulation experiments that
937 show NO_2^- oxidation at putative O_2 concentrations as low as 1 nM, an O_2 concentration so low
938 that the experimental conditions are functionally anoxic. We conducted experiments on waters
939 from two deoxygenated depths to evaluate if NO_2^- dismutation provides the oxidative power for
940 observed anaerobic NO_2^- oxidation and found no evidence of NO_2^- dismutation except in one
941 treatment – the closest to in situ NO_2^- conditions. Further exploration of the dismutation
942 hypothesis might therefore usefully focus on conditions near in situ NO_2^- concentrations. Across
943 our experiments, the percent of N loss due to anammox was consistently above the theoretical
944 prediction of at most 29% anammox. Our observations that NO_3^- reduction and NO_2^- oxidation
945 greatly surpass N loss, especially in shallow boundary waters, further reinforce the view that
946 NO_2^- in the SNM is sourced from NO_3^- reduction.

947 Together, these observations provide additional data that supports several new views of
948 OMZ biogeochemistry. However, additional work is especially needed to further validate the
949 occurrence of NO_2^- oxidation under functionally anoxic conditions, explore alternative oxidants
950 for this process, and comprehend how OMZ biogeochemistry could change with climate change
951 and other human-caused environmental changes.

952



953 **Author contributions**

954 XS, CF and BBW designed, and CF performed, measured, and calculated the NO_3^- reduction and
955 NH_4^+ oxidation rates. BBW and JCT designed, BBW and JCT performed, and JCT measured
956 and calculated the anammox and denitrification depth profile experiments. BBW and XS
957 designed, JCT, BBW, and XS performed, XS and KD measured, and KD, EW, and JCT
958 calculated the NO_2^- oxidation depth profiles. TT and ARB designed, TT performed, DEM and
959 JCT measured, and EW and JCT calculated the anammox and denitrification profiles from the
960 FK180624 cruise. TT and ARB designed, and TT performed, measured, and calculated the NO_2^-
961 oxidation O_2 variation experiments. SO provided critical help in running the mass spectrometer
962 to measure all samples except the oxygen variation experiments. BBW performed the
963 correlation and RDA analyses. JCT drafted the paper with inputs from all authors.

964

965 **Competing Interests**

966 The authors declare that they have no conflict of interest.

967

968 **Data Availability**

969 All data discussed in this manuscript will be archived in Zenodo upon publication.

970

971 **Acknowledgments**

972 We would like to acknowledge the crew and scientists of the R/V *Sally Ride* and the R/V *Falkor*
973 for logistical and scientific support during our 2018 cruises. We thank Amal Jayakumar for
974 providing *amoA* and *nirS* gene abundances for the RDA and PCA analyses. We thank Emilio
975 Robledo-Garcia for assistance using the LUMOS sensor for the NO_2^- oxidation O_2 gradient



976 experiments. We thank Matthias Spieler for supporting NO_3^- reduction rate measurements in
977 Basel. We also acknowledge the Schmidt Ocean Institute which provided R/V *Falkor* ship time
978 to ARB. We thank the Simons Foundation and National Science Foundation for supporting
979 ARB, TT, and DEM on Simons Foundation grant 622065 and NSF grants OCE-2138890 and
980 OCE-2142998 as well as support for BBW, CF, JCT, and XS through NSF grant OCE-1657663.

981

982 **References**

983 Anderson, J. J., Okubo, A., Robbins, A. S., and Richards, F. A.: A model for nitrate distributions
984 in oceanic oxygen minimum zones, *Deep Sea Res. Part A. Oceanogr. Res. Pap.*, 29, 1113–1140,
985 [https://doi.org/10.1016/0198-0149\(82\)90031-0](https://doi.org/10.1016/0198-0149(82)90031-0), 1982.

986 ASTM International: *Standard Guide for Spiking into Aqueous Samples*, West Conshohocken,
987 PA, 2006.

988 Babbin, A. R., Keil, R. G., Devol, A. H., and Ward, B. B.: Organic matter stoichiometry, flux,
989 and oxygen control nitrogen loss in the ocean, *Science* (80-.), 344, 406–408,
990 <https://doi.org/10.1126/science.1248364>, 2014.

991 Babbin, A. R., Peters, B. D., Mordy, C. W., Widner, B., Casciotti, K. L., and Ward, B. B.:
992 Multiple metabolisms constrain the anaerobic nitrite budget in the Eastern Tropical South
993 Pacific, *Global Biogeochem. Cycles*, 31, 258–271, <https://doi.org/10.1002/2016GB005407>,
994 2017.

995 Babbin, A. R., Buchwald, C., Morel, F. M. M., Wankel, S. D., and Ward, B. B.: Nitrite oxidation
996 exceeds reduction and fixed nitrogen loss in anoxic Pacific waters, *Mar. Chem.*, 224, 103814,
997 <https://doi.org/10.1016/J.MARCHEM.2020.103814>, 2020.

998 Bange, H. W., Rixen, T., Johansen, A. M., Siefert, R. L., Ramesh, R., Ittekkot, V., Hoffmann, M.



- 999 R., and Andreae, M. O.: A revised nitrogen budget of the Arabian Sea, *Global Biogeochem.*
1000 *Cycles*, 14, 1283–1297, <https://doi.org/10.1029/1999GB001228>, 2000.
- 1001 Beman, J. M., Leilei Shih, J., and Popp, B. N.: Nitrite oxidation in the upper water column and
1002 oxygen minimum zone of the eastern tropical North Pacific Ocean, *ISME J.* 2013 711, 7, 2192–
1003 2205, <https://doi.org/10.1038/ismej.2013.96>, 2013.
- 1004 Berg, J. S., Ahmerkamp, S., Pjevac, P., Hausmann, B., Milucka, J., and Kuypers, M. M. M.:
1005 How low can they go? Aerobic respiration by microorganisms under apparent anoxia, *FEMS*
1006 *Microbiol. Rev.*, 46, 1–14, <https://doi.org/10.1093/FEMSRE/FUAC006>, 2022.
- 1007 Bock, E., Koops, H. P., Möller, U. C., and Rudert, M.: A new facultatively nitrite oxidizing
1008 bacterium, *Nitrobacter vulgaris* sp. nov., *Arch. Microbiol.* 1990 1532, 153, 105–110,
1009 <https://doi.org/10.1007/BF00247805>, 1990.
- 1010 De Brabandere, L., Canfield, D. E., Dalsgaard, T., Friederich, G. E., Revsbech, N. P., Ulloa, O.,
1011 and Thamdrup, B.: Vertical partitioning of nitrogen-loss processes across the oxic-anoxic
1012 interface of an oceanic oxygen minimum zone, *Environ. Microbiol.*, 16, 3041–3054,
1013 <https://doi.org/10.1111/1462-2920.12255>, 2014.
- 1014 Braman, R. S. and Hendrix, S. A.: Nanogram Nitrite and Nitrate Determination in Environmental
1015 and Biological Materials by Vanadium(III) Reduction with Chemiluminescence Detection, *Anal.*
1016 *Chem.*, 61, 2715–2718, 1989.
- 1017 Brandes, J. A. and Devol, A. H.: A global marine-fixed nitrogen isotopic budget: Implications
1018 for Holocene nitrogen cycling, *Global Biogeochem. Cycles*, 16, 67–1,
1019 <https://doi.org/10.1029/2001GB001856>, 2002.
- 1020 Brandhorst, W.: Nitrification and Denitrification in the Eastern Tropical North Pacific, *J. du*
1021 *Cons. Cons. Perm. Int. pour l’exploration la mer*, 25, 3–20, 1959.



1022 Bristow, L. A., Dalsgaard, T., Tiano, L., Mills, D. B., Bertagnolli, A. D., Wright, J. J., Hallam, S.
1023 J., Ulloa, O., Canfield, D. E., Revsbech, N. P., and Thamdrup, B.: Ammonium and nitrite
1024 oxidation at nanomolar oxygen concentrations in oxygen minimum zone waters, *Proc. Natl.*
1025 *Acad. Sci. U. S. A.*, 113, 10601–10606, <https://doi.org/10.1073/PNAS.1600359113>, 2016.
1026 Bristow, L. A., Callbeck, C. M., Larsen, M., Altabet, M. A., Dekaezemacker, J., Forth, M.,
1027 Gauns, M., Glud, R. N., Kuypers, M. M. M., Lavik, G., Milucka, J., Naqvi, S. W. A., Pratihary,
1028 A., Revsbech, N. P., Thamdrup, B., Treusch, A. H., and Canfield, D. E.: N₂ production rates
1029 limited by nitrite availability in the Bay of Bengal oxygen minimum zone, *Nat. Geosci.*, 10, 24–
1030 29, <https://doi.org/10.1038/ngeo2847>, 2017.
1031 Buchwald, C. and Wankel, S. D.: Enzyme-catalyzed isotope equilibrium: A hypothesis to
1032 explain apparent N cycling phenomena in low oxygen environments, *Mar. Chem.*, 244, 104140,
1033 <https://doi.org/10.1016/J.MARCHEM.2022.104140>, 2022.
1034 Buchwald, C., Santoro, A. E., Stanley, R. H. R., and Casciotti, K. L.: Nitrogen cycling in the
1035 secondary nitrite maximum of the eastern tropical North Pacific off Costa Rica, *Global*
1036 *Biogeochem. Cycles*, 29, 2061–2081, <https://doi.org/10.1002/2015GB005187>, 2015.
1037 Bulow, S. E., Rich, J. J., Naik, H. S., Pratihary, A. K., and Ward, B. B.: Denitrification exceeds
1038 anammox as a nitrogen loss pathway in the Arabian Sea oxygen minimum zone, *Deep Sea Res.*
1039 *Part I Oceanogr. Res. Pap.*, 57, 384–393, <https://doi.org/10.1016/J.DSR.2009.10.014>, 2010.
1040 Busecke, J. J. M., Resplandy, L., Ditkovsky, S. J., and John, J. G.: Diverging Fates of the Pacific
1041 Ocean Oxygen Minimum Zone and Its Core in a Warming World, *AGU Adv.*, 3,
1042 e2021AV000470, <https://doi.org/10.1029/2021AV000470>, 2022.
1043 Casciotti, K. L.: Inverse kinetic isotope fractionation during bacterial nitrite oxidation, *Geochim.*
1044 *Cosmochim. Acta*, 73, 2061–2076, <https://doi.org/10.1016/J.GCA.2008.12.022>, 2009.



1045 Casciotti, K. L., Buchwald, C., and McIlvin, M.: Implications of nitrate and nitrite isotopic
1046 measurements for the mechanisms of nitrogen cycling in the Peru oxygen deficient zone, Deep
1047 Sea Res. Part I Oceanogr. Res. Pap., 80, 78–93, <https://doi.org/10.1016/J.DSR.2013.05.017>,
1048 2013.

1049 Codispoti, L. A.: An oceanic fixed nitrogen sink exceeding 400 Tg N a⁻¹ vs the concept of
1050 homeostasis in the fixed-nitrogen inventory, Biogeosciences, 4, 233–253,
1051 <https://doi.org/10.5194/BG-4-233-2007>, 2007.

1052 Codispoti, L. A. and Packard, T. T.: Denitrification rates in the eastern tropical South Pacific, J.
1053 Mar. Res., 38, 453–477, 1980.

1054 Codispoti, L. A. and Richards, F. A.: An analysis of the horizontal regime of denitrification in
1055 the eastern tropical North Pacific, Limnol. Oceanogr., 21, 379–388,
1056 <https://doi.org/10.4319/LO.1976.21.3.0379>, 1976.

1057 Codispoti, L. A., Brandes, J. A., Christensen, J. P., Devol, A. H., Naqvi, S. W. A., Paerl, H. W.,
1058 and Yoshinari, T.: The oceanic fixed nitrogen and nitrous oxide budgets: Moving targets as we
1059 enter the anthropocene?, Sci. Mar., 65, 85–105, <https://doi.org/10.3989/SCIMAR.2001.65S285>,
1060 2001.

1061 Codispoti, L. A., Yoshinari, T., and Devol, A. H.: Suboxic respiration in the oceanic water
1062 column, in: Respiration in Aquatic Ecosystems, edited by: del Giorgio, P. A. and Williams, P. J.
1063 L., Oxford University Press, 225–247, 2005.

1064 Dalsgaard, T., Canfield, D. E., Peterson, J., Thamdrup, B., and Acuna-Gonzales, J.: N production
1065 by anamox in the anoxic water column of Golfo Dulce, Costa Rica., Nature, 422, 606–608,
1066 <https://doi.org/10.1038/nature01526>, 2003.

1067 Dalsgaard, T., Thamdrup, B., Fariás, L., and Revsbech, N. P.: Anammox and denitrification in



1068 the oxygen minimum zone of the eastern South Pacific, *Limnol. Oceanogr.*, 57, 1331–1346,
1069 <https://doi.org/10.4319/lo.2012.57.5.1331>, 2012.

1070 Dalsgaard, T., Stewart, F. J., Thamdrup, B., De Brabandere, L., Revsbech, N. P., Ulloa, O.,
1071 Canfield, D. E., and Delong, E. F.: Oxygen at nanomolar levels reversibly suppresses process
1072 rates and gene expression in anammox and denitrification in the oxygen minimum zone off
1073 Northern Chile, *MBio*, 5, [https://doi.org/10.1128/MBIO.01966-](https://doi.org/10.1128/MBIO.01966-14/SUPPL_FILE/MBO005142028S1.PDF)
1074 [14/SUPPL_FILE/MBO005142028S1.PDF](https://doi.org/10.1128/MBIO.01966-14/SUPPL_FILE/MBO005142028S1.PDF), 2014.

1075 Freitag, A., Rudert, M., and Bock, E.: Growth of *Nitrobacter* by dissimilatoric nitrate reduction,
1076 *FEMS Microbiol. Lett.*, 48, 105–109, <https://doi.org/10.1111/J.1574-6968.1987.TB02524.X>,
1077 1987.

1078 Frey, C., Bange, H. W., Achterberg, E. P., Jayakumar, A., Löscher, C. R., Arévalo-Martínez, D.
1079 L., León-Palmero, E., Sun, M., Sun, X., Xie, R. C., Oleynik, S., and Ward, B. B.: Regulation of
1080 nitrous oxide production in low-oxygen waters off the coast of Peru, *Biogeosciences*, 17, 2263–
1081 2287, <https://doi.org/10.5194/BG-17-2263-2020>, 2020.

1082 Frey, C., Sun, X., Szemlerski, L., Casciotti, K. L., Garcia-Robledo, E., Jayakumar, A., Kelly, C.
1083 L., and Lehmann, M. F.: Nitrous oxide production kinetics from ammonia oxidation in the
1084 Eastern Tropical North Pacific, *Limnol. Oceanogr.*, Under review, 2022.

1085 Fuchsman, C. A., Devol, A. H., Saunders, J. K., McKay, C., and Rocap, G.: Niche partitioning of
1086 the N cycling microbial community of an offshore oxygen deficient zone, *Front. Microbiol.*, 8,
1087 2384, <https://doi.org/10.3389/FMICB.2017.02384/BIBTEX>, 2017.

1088 Füssel, J., Lam, P., Lavik, G., Jensen, M. M., Holtappels, M., Günter, M., and Kuypers, M. M.
1089 M.: Nitrite oxidation in the Namibian oxygen minimum zone, *ISME J.*, 6, 1200–1209,
1090 <https://doi.org/10.1038/ismej.2011.178>, 2011.



- 1091 Füssel, J., Lücker, S., Yilmaz, P., Nowka, B., van Kessel, M. A. H. J., Bourceau, P., Hach, P. F.,
1092 Littmann, S., Berg, J., Spieck, E., Daims, H., Kuypers, M. M. M., and Lam, P.: Adaptability as
1093 the key to success for the ubiquitous marine nitrite oxidizer *Nitrococcus*, *Sci. Adv.*, 3,
1094 https://doi.org/10.1126/SCIADV.1700807/SUPPL_FILE/1700807_TABLES1_TO_S10.ZIP,
1095 2017.
- 1096 Ganesh, S., Bristow, L. A., Larsen, M., Sarode, N., Thamdrup, B., and Stewart, F. J.: Size-
1097 fraction partitioning of community gene transcription and nitrogen metabolism in a marine
1098 oxygen minimum zone, *ISME J.* 2015 912, 9, 2682–2696, <https://doi.org/10.1038/ismej.2015.44>,
1099 2015.
- 1100 Garcia-Robledo, E., Padilla, C. C., Aldunate, M., Stewart, F. J., Ulloa, O., Paulmier, A., Gregori,
1101 G., and Revsbech, N. P.: Cryptic oxygen cycling in anoxic marine zones, *Proc. Natl. Acad. Sci.*
1102 *U. S. A.*, 114, 8319–8324, <https://doi.org/10.1073/PNAS.1619844114>, 2017.
- 1103 Granger, J., & Sigman, D. M.: Removal of nitrite with sulfamic acid for nitrate N and O isotope
1104 analysis with the denitrifier method, *Rapid Commun. Mass Spectrom.*, 23, 3753–3762., *Rapid*
1105 *Commun. Mass Spectrom.*, 23, 3753–3762, <https://doi.org/10.1002/rcm>, 2009.
- 1106 Granger, J. and Wankel, S. D.: Isotopic overprinting of nitrification on denitrification as a
1107 ubiquitous and unifying feature of environmental nitrogen cycling, *Proc. Natl. Acad. Sci. U. S.*
1108 *A.*, 113, E6391–E6400,
1109 https://doi.org/10.1073/PNAS.1601383113/SUPPL_FILE/PNAS.201601383SI.PDF, 2016.
- 1110 Gruber, N.: The Dynamics of the Marine Nitrogen Cycle and its Influence on Atmospheric CO
1111 Variations, in: *The Ocean Carbon Cycle and Climate*, 97–148, <https://doi.org/10.1007/978-1->
1112 [4020-2087-2_4](https://doi.org/10.1007/978-1-4020-2087-2_4), 2004.
- 1113 Hamersley, M. R., Lavik, G., Wobken, D., Rattray, J. E., Lam, P., Hopmans, E. C., Sinninghe



- 1114 Damsté, J. S., Krüger, S., Graco, M., Gutiérrez, D., and Kuypers, M. M. M.: Anaerobic
1115 ammonium oxidation in the Peruvian oxygen minimum zone, *Limnol. Oceanogr.*, 52, 923–933,
1116 <https://doi.org/10.4319/LO.2007.52.3.0923>, 2007.
- 1117 Holmes, R. M., Aminot, A., Kérouel, R., Hooker, B. A., and Peterson, B. J.: A simple and
1118 precise method for measuring ammonium in marine and freshwater ecosystems, *Can. J. Fish.*
1119 *Aquat. Sci.*, 56, 1801–1808, <https://doi.org/10.1139/f99-128>, 1999.
- 1120 Horak, R. E. A., Ruef, W., Ward, B. B., and Devol, A. H.: Expansion of denitrification and
1121 anoxia in the eastern tropical North Pacific from 1972 to 2012, *Geophys. Res. Lett.*, 43, 5252–
1122 5260, <https://doi.org/10.1002/2016GL068871>, 2016.
- 1123 Jayakumar, A., Wajih, S., Naqvi, A., and Ward, B. B.: Distribution and Relative Quantification
1124 of Key Genes Involved in Fixed Nitrogen Loss From the Arabian Sea Oxygen Minimum Zone,
1125 *Indian Ocean Biogeochem. Process. Ecol. Var. Geophys. Monogr. Ser.*, 185,
1126 <https://doi.org/10.1029/2008GM000730>, 2009.
- 1127 Jensen, M. M., Kuypers, M. M. M., Lavik, G., and Thamdrup, B.: Rates and regulation of
1128 anaerobic ammonium oxidation and denitrification in the Black Sea, *Limnol. Oceanogr.*, 53, 23–
1129 36, <https://doi.org/10.4319/LO.2008.53.1.0023>, 2008.
- 1130 Jensen, M. M., Lam, P., Revsbech, N. P., Nagel, B., Gaye, B., Jetten, M. S. M., and Kuypers, M.
1131 M. M.: Intensive nitrogen loss over the Omani Shelf due to anammox coupled with dissimilatory
1132 nitrite reduction to ammonium, *ISME J.* 2011 510, 5, 1660–1670,
1133 <https://doi.org/10.1038/ismej.2011.44>, 2011.
- 1134 Kalvelage, T., Jensen, M. M., Contreras, S., Revsbech, N. P., Lam, P., Günter, M., LaRoche, J.,
1135 Lavik, G., and Kuypers, M. M. M.: Oxygen Sensitivity of Anammox and Coupled N-Cycle
1136 Processes in Oxygen Minimum Zones, *PLoS One*, 6, e29299,



- 1137 <https://doi.org/10.1371/JOURNAL.PONE.0029299>, 2011.
- 1138 Kalvelage, T., Lavik, G., Lam, P., Contreras, S., Arteaga, L., Löscher, C. R., Oschlies, A.,
1139 Paulmier, A., Stramma, L., and M Kuypers, M. M.: Nitrogen cycling driven by organic matter
1140 export in the South Pacific oxygen minimum zone, 55812, <https://doi.org/10.1038/NGEO1739>,
1141 2013.
- 1142 Keeling, R. F., Körtzinger, A., and Gruber, N.: Ocean deoxygenation in a warming world, *Ann.*
1143 *Rev. Mar. Sci.*, 2, 199–229, <https://doi.org/10.1146/annurev.marine.010908.163855>, 2010.
- 1144 Kemeny, P. C., Weigand, M. A., Zhang, R., Carter, B. R., Karsh, K. L., Fawcett, S. E., and
1145 Sigman, D. M.: Enzyme-level interconversion of nitrate and nitrite in the fall mixed layer of the
1146 Antarctic Ocean, *Global Biogeochem. Cycles*, 30, 1069–1085,
1147 <https://doi.org/10.1002/2015GB005350>, 2016.
- 1148 Kirstein, K. and Bock, E.: Close genetic relationship between *Nitrobacter hamburgensis* nitrite
1149 oxidoreductase and *Escherichia coli* nitrate reductases, *Arch. Microbiol.* 1993 1606, 160, 447–
1150 453, <https://doi.org/10.1007/BF00245305>, 1993.
- 1151 Koch, H., Lücker, S., Albertsen, M., Kitzinger, K., Herbold, C., Spieck, E., Nielsen, P. H.,
1152 Wagner, M., and Daims, H.: Expanded metabolic versatility of ubiquitous nitrite-oxidizing
1153 bacteria from the genus *Nitrospira*, *Proc. Natl. Acad. Sci. U. S. A.*, 112, 11371–11376,
1154 <https://doi.org/10.1073/PNAS.1506533112>, 2015.
- 1155 Kondo, Y. and Moffett, J. W.: Iron redox cycling and subsurface offshore transport in the eastern
1156 tropical South Pacific oxygen minimum zone, *Mar. Chem.*, 168, 95–103,
1157 <https://doi.org/10.1016/J.MARCHEM.2014.11.007>, 2015.
- 1158 Kraft, B., Jehmlich, N., Larsen, M., Bristow, L. A., Könneke, M., Thamdrup, B., and Canfield,
1159 D. E.: Oxygen and nitrogen production by an ammonia-oxidizing archaeon, *Science* (80-.), 375,



1160 97–100,
1161 https://doi.org/10.1126/SCIENCE.ABE6733/SUPPL_FILE/SCIENCE.ABE6733_MDAR_REPR
1162 [ODUCIBILITY_CHECKLIST.PDF](#), 2022.
1163 Kuenen, J. G.: Anammox bacteria from discovery, 6, <https://doi.org/10.1038/nrmicro1857>, 2008.
1164 Kuypers, M. M. M., Lavik, G., Woebken, D., Schmid, M., Fuchs, B. M., Amann, R., Jørgensen,
1165 B. B., and Jetten, M. S. M.: Massive nitrogen loss from the Benguela upwelling system through
1166 anaerobic ammonium oxidation, *Proc. Natl. Acad. Sci. U. S. A.*, 102, 6478–6483,
1167 <https://doi.org/10.1073/PNAS.0502088102>, 2005.
1168 Lam, P. and Kuypers, M. M. M.: Microbial Nitrogen Cycling Processes in Oxygen Minimum
1169 Zones, *Ann. Rev. Mar. Sci.*, 3, 317–345, <https://doi.org/10.1146/annurev-marine-120709->
1170 142814, 2011.
1171 Lam, P., Lavik, G., Jensen, M. M., Van Vossenberg, J. De, Schmid, M., Woebken, D., Gutiérrez,
1172 D., Amann, R., Jetten, M. S. M., and Kuypers, M. M. M.: Revising the nitrogen cycle in the
1173 Peruvian oxygen minimum zone, *Proc. Natl. Acad. Sci. U. S. A.*, 106, 4752–4757,
1174 <https://doi.org/10.1073/PNAS.0812444106>, 2009.
1175 Lam, P., Jensen, M. M., Kock, A., Lettmann, K. A., Plancherel, Y., Lavik, G., Bange, H. W., and
1176 Kuypers, M. M. M.: Origin and fate of the secondary nitrite maximum in the Arabian Sea,
1177 *Biogeosciences*, 8, 1565–1577, <https://doi.org/10.5194/BG-8-1565-2011>, 2011.
1178 Van de Leemput, I. A., Veraart, A. J., Dakos, V., De Klein, J. J. M., Strous, M., and Scheffer,
1179 M.: Predicting microbial nitrogen pathways from basic principles, *Environ. Microbiol.*, 13,
1180 1477–1487, <https://doi.org/10.1111/J.1462-2920.2011.02450.X>, 2011.
1181 Lehner, P., Larndorfer, C., Garcia-Robledo, E., Larsen, M., Borisov, S. M., Revsbech, N. P.,
1182 Glud, R. N., Canfield, D. E., and Klimant, I.: LUMOS - A Sensitive and Reliable Optode System



1183 for Measuring Dissolved Oxygen in the Nanomolar Range, PLoS One, 10, e0128125,
1184 <https://doi.org/10.1371/JOURNAL.PONE.0128125>, 2015.

1185 Lipschultz, F., Wofsy, S. C., Ward, B. B., Codispoti, L. A., Friedrich, G., and Elkins, J. W.:
1186 Bacterial transformations of inorganic nitrogen in the oxygen-deficient waters of the Eastern
1187 Tropical South Pacific Ocean, Deep Sea Res. Part A. Oceanogr. Res. Pap., 37, 1513–1541,
1188 [https://doi.org/10.1016/0198-0149\(90\)90060-9](https://doi.org/10.1016/0198-0149(90)90060-9), 1990.

1189 Lomas, M. W. and Lipschultz, F.: Forming the primary nitrite maximum: Nitrifiers or
1190 phytoplankton?, Limnol. Oceanogr., 51, 2453–2467, <https://doi.org/10.4319/LO.2006.51.5.2453>,
1191 2006.

1192 Luther, G. W.: The role of one- and two-electron transfer reactions in forming
1193 thermodynamically unstable intermediates as barriers in multi-electron redox reactions, Aquat.
1194 Geochemistry, 16, 395–420, <https://doi.org/10.1007/S10498-009-9082-3/FIGURES/14>, 2010.

1195 Luther, G. W. and Popp, J. I.: Kinetics of the Abiotic Reduction of Polymeric Manganese
1196 Dioxide by Nitrite: An Anaerobic Nitrification Reaction, Aquat. Geochemistry 2002 81, 8, 15–
1197 36, <https://doi.org/10.1023/A:1020325604920>, 2002.

1198 Martin, J. H., Knauer, G. A., Karl, D. M., and Broenkow, W. W.: VERTEX: carbon cycling in
1199 the northeast Pacific, Deep Sea Res. Part A. Oceanogr. Res. Pap., 34, 267–285,
1200 [https://doi.org/10.1016/0198-0149\(87\)90086-0](https://doi.org/10.1016/0198-0149(87)90086-0), 1987.

1201 McIlvin, M. R. and Altabet, M. A.: Chemical conversion of nitrate and nitrite to nitrous oxide for
1202 nitrogen and oxygen isotopic analysis in freshwater and seawater, Anal. Chem., 77, 5589–5595,
1203 <https://doi.org/10.1021/ac050528s>, 2005.

1204 Mincer, T. J., Church, M. J., Taylor, L. T., Preston, C., Karl, D. M., and DeLong, E. F.:
1205 Quantitative distribution of presumptive archaeal and bacterial nitrifiers in Monterey Bay and the



- 1206 North Pacific Subtropical Gyre, *Environ. Microbiol.*, 9, 1162–1175,
1207 <https://doi.org/10.1111/J.1462-2920.2007.01239.X>, 2007.
- 1208 Moriyasu, R., Evans, N., Bolster, K. M., Hardisty, D. S., and Moffett, J. W.: The Distribution
1209 and Redox Speciation of Iodine in the Eastern Tropical North Pacific Ocean, *Global*
1210 *Biogeochem. Cycles*, 34, e2019GB006302, <https://doi.org/10.1029/2019GB006302>, 2020.
- 1211 Naqvi, S. W. A.: Some aspects of the oxygen-deficient conditions and denitrification in the
1212 Arabian Sea, *J. Mar. Res.*, 45, 1049–1072, 1987.
- 1213 Nozaki, Y.: A fresh look at element distribution in the North Pacific Ocean, *Eos, Trans. Am.*
1214 *Geophys. Union*, 78, 221–221, <https://doi.org/10.1029/97EO00148>, 1997.
- 1215 Oshiki, M., Satoh, H., and Okabe, S.: Ecology and physiology of anaerobic ammonium oxidizing
1216 bacteria, *Environ. Microbiol.*, 18, 2784–2796, [https://doi.org/10.1111/1462-](https://doi.org/10.1111/1462-2920.13134)
1217 [2920.13134](https://doi.org/10.1111/1462-2920.13134)/SUPPINFO, 2016.
- 1218 Padilla, C. C., Bristow, L. A., Sarode, N., Garcia-Robledo, E., Gómez Ramírez, E., Benson, C.
1219 R., Bourbonnais, A., Altabet, M. A., Girguis, P. R., Thamdrup, B., and Stewart, F. J.: NC10
1220 bacteria in marine oxygen minimum zones, *ISME J.* 2016 108, 10, 2067–2071,
1221 <https://doi.org/10.1038/ismej.2015.262>, 2016.
- 1222 Peng, X., Fuchsman, C. A., Jayakumar, A., Oleynik, S., Martens-Habbena, W., Devol, A. H., and
1223 Ward, B. B.: Ammonia and nitrite oxidation in the Eastern Tropical North Pacific, *Global*
1224 *Biogeochem. Cycles*, 29, 2034–2049, <https://doi.org/10.1002/2015GB005278>, 2015.
- 1225 Peng, X., Fuchsman, C. A., Jayakumar, A., Warner, M. J., Devol, A. H., and Ward, B. B.:
1226 Revisiting nitrification in the Eastern Tropical South Pacific: A focus on controls, *J. Geophys.*
1227 *Res. Ocean.*, 121, 1667–1684, <https://doi.org/10.1002/2015JC011455>, 2016.
- 1228 Penn, J., Weber, T., and Deutsch, C.: Microbial functional diversity alters the structure and



1229 sensitivity of oxygen deficient zones, *Geophys. Res. Lett.*, 43, 9773–9780,
1230 <https://doi.org/10.1002/2016GL070438>, 2016.

1231 Peters, B. D., Babbin, A. R., Lettmann, K. A., Mordy, C. W., Ulloa, O., Ward, B. B., and
1232 Casciotti, K. L.: Vertical modeling of the nitrogen cycle in the eastern tropical South Pacific
1233 oxygen deficient zone using high-resolution concentration and isotope measurements, *Global*
1234 *Biogeochem. Cycles*, 30, 1661–1681, <https://doi.org/10.1002/2016GB005415>, 2016.

1235 R: A language and environment for statistical computing:
1236 Starkenburg, S. R., Larimer, F. W., Stein, L. Y., Klotz, M. G., Chain, P. S. G., Sayavedra-Soto,
1237 L. A., Poret-Peterson, A. T., Gentry, M. E., Arp, D. J., Ward, B., and Bottomley, P. J.: Complete
1238 genome sequence of *Nitrobacter hamburgensis* X14 and comparative genomic analysis of
1239 species within the genus *Nitrobacter*, *Appl. Environ. Microbiol.*, 74, 2852–2863,
1240 https://doi.org/10.1128/AEM.02311-07/SUPPL_FILE/SUPPLEMENTAL_TABLE_2.PDF,
1241 2008.

1242 Stramma, L., Johnson, G. C., Sprintall, J., and Mohrholz, V.: Expanding oxygen-minimum zones
1243 in the tropical oceans, *Science* (80-.), 320, 655–658,
1244 [https://doi.org/10.1126/SCIENCE.1153847/ASSET/09F7EF41-9228-40BD-8E17-
1245 06C4E9218CC5/ASSETS/GRAPHIC/320_655_F2.JPEG](https://doi.org/10.1126/SCIENCE.1153847/ASSET/09F7EF41-9228-40BD-8E17-06C4E9218CC5/ASSETS/GRAPHIC/320_655_F2.JPEG), 2008.

1246 Strickland, J. D. H. and Parsons, T. R.: *A Practical Handbook of Seawater Analysis*, Fisheries
1247 Research Board of Canada, Ottawa, 1972.

1248 Strohm, T. O., Griffin, B., Zumft, W. G., and Schink, B.: Growth yields in bacterial
1249 denitrification and nitrate ammonification, *Appl. Environ. Microbiol.*, 73, 1420–1424,
1250 [https://doi.org/10.1128/AEM.02508-06/ASSET/88AA1997-7BB3-42B6-A761-
1251 DCB47D972CA6/ASSETS/GRAPHIC/ZAM0050775730001.JPEG](https://doi.org/10.1128/AEM.02508-06/ASSET/88AA1997-7BB3-42B6-A761-DCB47D972CA6/ASSETS/GRAPHIC/ZAM0050775730001.JPEG), 2007.



1252 Strous, M., Heijnen, J. J., Kuenen, J. G., and Jetten, M. S. M.: The sequencing batch reactor as a
1253 powerful tool for the study of slowly growing anaerobic ammonium-oxidizing microorganisms,
1254 *Appl. Microbiol. Biotechnol.* 1998 505, 50, 589–596, <https://doi.org/10.1007/S002530051340>,
1255 1998.

1256 Sun, X. and Ward, B. B.: Novel metagenome-assembled genomes involved in the nitrogen cycle
1257 from a Pacific oxygen minimum zone, *ISME Commun.* 2021 11, 1, 1–5,
1258 <https://doi.org/10.1038/s43705-021-00030-2>, 2021.

1259 Sun, X., Ji, Q., Jayakumar, A., and Ward, B. B.: Dependence of nitrite oxidation on nitrite and
1260 oxygen in low-oxygen seawater, *Geophys. Res. Lett.*, 44, 7883–7891,
1261 <https://doi.org/10.1002/2017GL074355>, 2017.

1262 Sun, X., Kop, L. F. M., Lau, M. C. Y., Frank, J., Jayakumar, A., Lücker, S., and Ward, B. B.:
1263 Uncultured Nitrospina-like species are major nitrite oxidizing bacteria in oxygen minimum
1264 zones, *ISME J.*, <https://doi.org/10.1038/s41396-019-0443-7>, 2019.

1265 Sun, X., Frey, C., Garcia-Robledo, E., Jayakumar, A., and Ward, B. B.: Microbial niche
1266 differentiation explains nitrite oxidation in marine oxygen minimum zones, *ISME J.* 2021 155,
1267 15, 1317–1329, <https://doi.org/10.1038/s41396-020-00852-3>, 2021.

1268 Tang, W., Tracey, J. C., Carroll, J., Wallace, E., Lee, J. A., Nathan, L., Sun, X., Jayakumar, A.,
1269 and Ward, B. B.: Nitrous oxide production in the Chesapeake Bay, *Limnol. Oceanogr.*, 67,
1270 2101–2116, <https://doi.org/10.1002/LNO.12191>, 2022.

1271 Taylor, B. W., Keep, C. F., Hall, R. O., Koch, B. J., Tronstad, L. M., Flecker, A. S., and Ulseth,
1272 A. J.: Improving the fluorometric ammonium method: matrix effects, background fluorescence,
1273 and standard additions, *Am. Benthol. Soc.*, 26, 167–177, <https://doi.org/10.1899/0887-3593>,
1274 2007.



- 1275 Thamdrup, B. and Dalsgaard, T.: The fate of ammonium in anoxic manganese oxide-rich marine
1276 sediment, *Geochim. Cosmochim. Acta*, 64, 4157–4164, <https://doi.org/10.1016/S0016->
1277 7037(00)00496-8, 2000.
- 1278 Thamdrup, B. and Dalsgaard, T.: Production of N₂ through anaerobic ammonium oxidation
1279 coupled to nitrate reduction in marine sediments, *Appl. Environ. Microbiol.*, 68, 1312–1318,
1280 <https://doi.org/10.1128/AEM.68.3.1312-1318.2002/ASSET/F1579424-64C0-464C-AF9C->
1281 5BEB3458C869/ASSETS/GRAPHIC/AM0321630005.JPEG, 2002.
- 1282 Thamdrup, B., Dalsgaard, T., Jensen, M. M., Ulloa, O., Farías, L., and Escribano, R.: Anaerobic
1283 ammonium oxidation in the oxygen-deficient waters off northern Chile, *Limnol. Oceanogr.*, 51,
1284 2145–2156, <https://doi.org/10.4319/LO.2006.51.5.2145>, 2006.
- 1285 Tiano, L., Garcia-Robledo, E., Dalsgaard, T., Devol, A. H., Ward, B. B., Ulloa, O., Canfield, D.
1286 E., and Peter Revsbech, N.: Oxygen distribution and aerobic respiration in the north and south
1287 eastern tropical Pacific oxygen minimum zones, *Deep Sea Res. Part I Oceanogr. Res. Pap.*, 94,
1288 173–183, <https://doi.org/10.1016/J.DSR.2014.10.001>, 2014.
- 1289 Tsementzi, D., Wu, J., Deutsch, S., Nath, S., Rodriguez-R, L. M., Burns, A. S., Ranjan, P.,
1290 Sarode, N., Malmstrom, R. R., Padilla, C. C., Stone, B. K., Bristow, L. A., Larsen, M., Glass, J.
1291 B., Thamdrup, B., Woyke, T., Konstantinidis, K. T., and Stewart, F. J.: SAR11 bacteria linked to
1292 ocean anoxia and nitrogen loss, *Nature*, 536, 179–183, <https://doi.org/10.1038/nature19068>,
1293 2016.
- 1294 Ulloa, O., Canfield, D. E., DeLong, E. F., Letelier, R. M., and Stewart, F. J.: Microbial
1295 oceanography of anoxic oxygen minimum zones, *Proc. Natl. Acad. Sci. U. S. A.*, 109, 15996–
1296 16003, <https://doi.org/10.1073/PNAS.1205009109>, 2012.
- 1297 Vedamati, J., Chan, C., and Moffett, J. W.: Distribution of dissolved manganese in the Peruvian



1298 Upwelling and Oxygen Minimum Zone, *Geochim. Cosmochim. Acta*, 156, 222–240,
1299 <https://doi.org/10.1016/J.GCA.2014.10.026>, 2015.

1300 Wanninkhof, R.: Relationship between wind speed and gas exchange over the ocean, *J. Geophys.*
1301 *Res. Ocean.*, 97, 7373–7382, <https://doi.org/10.1029/92JC00188>, 1992.

1302 Ward, B. B., Glover, H. E., and Lipschultz, F.: Chemoautotrophic activity and nitrification in the
1303 oxygen minimum zone off Peru, *Deep Sea Res. Part A. Oceanogr. Res. Pap.*, 36, 1031–1051,
1304 [https://doi.org/10.1016/0198-0149\(89\)90076-9](https://doi.org/10.1016/0198-0149(89)90076-9), 1989.

1305 Ward, B. B., Tuit, C. B., Jayakumar, A., Rich, J. J., Moffett, J., and Naqvi, S. W. A.: Organic
1306 carbon, and not copper, controls denitrification in oxygen minimum zones of the ocean, *Deep*
1307 *Sea Res. Part I Oceanogr. Res. Pap.*, 55, 1672–1683, <https://doi.org/10.1016/J.DSR.2008.07.005>,
1308 2008.

1309 Ward, B. B., Devol, A. H., Rich, J. J., Chang, B. X., Bulow, S. E., Naik, H., Pratihary, A., and
1310 Jayakumar, A.: Denitrification as the dominant nitrogen loss process in the Arabian Sea, *Nat.*
1311 2009 4617260, 461, 78–81, <https://doi.org/10.1038/nature08276>, 2009.

1312 Weigand, M. A., Foriel, J., Barnett, B., Oleynik, S., and Sigman, D. M.: Updates to
1313 instrumentation and protocols for isotopic analysis of nitrate by the denitrifier method, *Rapid*
1314 *Commun. Mass Spectrom.*, 30, 1365–1383, <https://doi.org/10.1002/rcm.7570>, 2016.

1315 Wunderlich, A., Meckenstock, R. U., and Einsiedl, F.: A mixture of nitrite-oxidizing and
1316 denitrifying microorganisms affects the $\delta^{18}\text{O}$ of dissolved nitrate during anaerobic microbial
1317 denitrification depending on the $\delta^{18}\text{O}$ of ambient water, *Geochim. Cosmochim. Acta*, 119, 31–
1318 45, <https://doi.org/10.1016/J.GCA.2013.05.028>, 2013.

1319